DEPARTMENT OF PHYSICS
UNIVERSITY OF JYVÄSKYLÄ
RESEARCH REPORT No. 2/2008

STUDIES OF STERILE NEUTRINOS IN ASTROPHYSICS

BY
MINJA HÄNNINEN

Academic Dissertation
for the Degree of
Doctor of Philosophy

To be presented, by permission of the
Faculty of Mathematics and Natural Sciences
of the University of Jyväskylä,
for public examination in Auditorium FYS-1 of the
University of Jyväskylä on February 29, 2008
at 12 o'clock noon

Jyväskylä, Finland
February 2008

ISBN 978-951-39-3193-3
URN:ISBN:978-951-39-3193-3

Preface

I never believed to do a PhD some day. I owe several persons a debt. First of all, I wish to thank my supervisor Professor Jukka Maalampi for all his help and patience, not to mention his open-mindedness to give me an opportunity to begin studies in a field unfamiliar to me. It has been a pleasure to work with Docent Petteri Keränen and MSc Janne Riittinen. I appreciate their invaluable help and co-operation in this study, and also the refreshing moments in spare time, when science has been temporarily put into background. I should also mention Docent Kimmo Kainulainen, who has kindly shared his knowledge in cosmology related subjects.

I have really enjoyed working at Department of Physics. I have got help every time I have bothered to ask. Thanks to you all. Especially, without the kind help of administrative staff in practicalities I would have given up several times.

I am grateful to Professor Tapio Rantala from Tampere University of Technology for helping me with my beginnings in science. MSc Pasi Ahtola was the important person who encouraged me to move on to particle physics and to continue my studies at Jyväskylä.

University of Jyväskylä, Graduate School of Particle and Nuclear Physics and Finnish Cultural Foundation has offered financial support for this thesis. I gratefully acknowledge them, as well as the hospitality of Nordita.

Thanks for everyone with whom I have spent spare time during these years. Luckily you are too many to mention by name. I am most grateful to my parents, who have supported me in many ways during my studies. Last I wish to express my gratitude to Aleksi, who has given me faith that there is still life after this thesis.

Jyväskylä, January 2008

Minja Hänninen

Abstract

This thesis considers the possibility that besides the three neutrinos in the Standard Model (SM) there exist one or more sterile neutrinos which lack the SM gauge interactions. Many extensions of the SM predict sterile neutrinos, but so far their existence has not been confirmed by neutrino oscillation experiments. In this study it is assumed that three sterile neutrinos exist and that they mix pairwise with three superpositions (the mass eigenstates of neutrinos in the SM) of the active neutrinos ν_e, ν_μ and ν_τ. The mass-squared differences between mass eigenstates in each pair are assumed to be so small that the existence of the new states would not have affected the results of the neutrino experiments performed so far. It is shown that neutrinos from distant astrophysical sources, like supernovae and Active Galactic Nuclei (AGN), provide an excellent tool for studying this kind of neutrino spectrum.

Ultrahigh-energy neutrinos produced in AGN may oscillate into sterile states during their flight to the Earth. It is shown that it would have notable effects on the ratios of ordinary neutrino fluxes measured at the Earth. In core collapse supernovae sterile neutrinos may be generated via matter effects when neutrinos born in supernova core traverse the medium with decreasing density to the surface of the star. The behavior of neutrinos in supernova is explored both numerically and by using the Landau-Zener approximation.

The Landau-Zener theory considers transitions in two-level quantum systems with a linear time dependence and it cannot be directly applied to the neutrino system of supernovae. Supernovae have nonlinear profiles and three differently interacting neutrino types (ν_e, $\nu_{\mu,\tau}$, ν_s) have different effective potential energies in matter. A general solution to such nonlinear multistate system do not exist. Probabilities for some specific transitions in a multistate linear system are known to be calculable by using the two-state Landau-Zener probabilities, even when the transitions do not occur independently. The applicability of this independent crossing approximation for nonlinear case is tested in this thesis and it is found to apply reasonably well.

List of publications

I P. Keränen, J. Maalampi, M. Myyryläinen and J. Riittinen, *Effects of sterile neutrinos on the ultrahigh-energy cosmic neutrino flux*, Phys. Lett. B 574 (2003) 162

II P. Keränen, J. Maalampi, M. Myyryläinen and J. Riittinen, *Effects of degenerate sterile neutrinos on the supernova neutrino flux*, Phys. Lett. B 597 (2004) 374

III P. Keränen, J. Maalampi, M. Myyryläinen and J. Riittinen, *Landau-Zener problem in a three-level neutrino system with nonlinear time dependence*, Phys. Rev. D 75 (2007) 033006

IV P. Keränen, J. Maalampi, M. Myyryläinen and J. Riittinen, *Sterile neutrino signals from supernovae*, Phys. Rev. D 76 (2007) 125026

The author (née Myyryläinen) has participated the preparation of all the papers and has written the draft versions of papers III and IV where she can be considered as the main author. The author is responsible for all the numerical calculations of the papers.

Contents

1 Neutrinos in standard model and beyond **1**
1.1 Neutrinos in vacuum . . . 2
1.1.1 Neutrino mixing in vacuum . . . 2
1.1.2 Neutrino oscillations in vacuum . . . 4
1.2 Neutrinos in matter . . . 6
1.2.1 The MSW effect . . . 7
1.3 Sterile neutrinos . . . 8

2 Neutrinos from astrophysical sources **13**
2.1 Solar neutrinos . . . 13
2.2 UHECR neutrinos . . . 16
2.3 Supernova neutrinos . . . 18

3 Landau-Zener theory and its extensions **23**
3.1 Level crossing problem for a two-state system . . . 24
3.2 Parametrization for LZ problem in neutrino physics . . . 25
3.3 Multistate linear system and ICA . . . 27

4 Effects of sterile neutrinos **29**
4.1 Model with nearly degenerate sterile neutrinos . . . 29
4.2 Effect on UHECR neutrino fluxes . . . 31
4.3 Effect on supernova neutrino fluxes . . . 34
4.4 Validity of ICA for three states in nonlinear potential . . . 40

Summary **45**

Chapter 1

Neutrinos in standard model and beyond

Neutrinos are weakly interacting uncharged particles. They are very light, but according to experimental data they are not strictly massless. The absolute mass scale value of neutrinos is unknown, but it is known to be orders of magnitude smaller than the masses of other particles. Neutrino masses are generated by a so far unknown mechanism.

The evidence of neutrino mass comes from the oscillation phenomena observed in connection to neutrinos created in nuclear reactions in the Sun and by cosmic rays in the atmosphere and also to neutrinos man-made in nuclear reactors. There are two conditions for the neutrino oscillations to happen. The first condition is that neutrinos have mass, or to be more specific, the difference between squared masses of two eigenstates must be nonzero. The second condition is that neutrinos are mixed, meaning that the states of propagation or the eigenstates of Hamiltonian, the so-called mass eigenstates, do not coincide with the states in terms of which the weak interactions are defined, the so-called weak interaction eigenstates, ν_e, ν_μ and ν_τ.

Neutrino oscillations violate the lepton number conservation. Neutrino flavor may also change when neutrinos travel in a medium. In matter the interactions of neutrinos with background matter, which are different for different flavors, modify the Hamiltonian and the eigenstates of neutrinos. The oscillation properties of neutrinos change, and in the case of a varying matter density enhanced flavor transitions may take place in certain density regions, called resonance regions.

Many extensions of the Standard Model (SM) of particle interactions predict existence of

one or more sterile neutrinos. Sterile neutrinos lack weak interactions but they can mix with ordinary neutrinos due to mass terms. Sterile neutrinos might be produced via neutrino oscillation or via matter effects.

1.1 Neutrinos in vacuum

1.1.1 Neutrino mixing in vacuum

The neutrino flavor states ν_l ($l = e, \mu, \tau, \dots$) are defined as states which interact via charged current interactions with corresponding charged lepton l. The neutrino mass states ν_j ($j = 1, 2, 3, \dots$) with masses m_j are the eigenstates of the total Hamiltonian in vacuum [1]. The measurement of the width of the decay $Z \to \nu\bar{\nu}$ at LEP experiment has set the number of ordinary-type neutrino flavors into three [2]. If additional massive neutrinos exist, they must be sterile, meaning that they do not couple to Z-boson. Correspondingly the ordinary neutrinos having the Standard Model gauge interactions are called active. Mass eigenstates do not coincide with the flavor states when the mass part of the Hamiltonian is not diagonal in flavor. Neutrinos are said to mix, and this vacuum mixing is described by the relation

$$|\nu_l\rangle = \sum_j U^*_{lj} |\nu_j\rangle. \tag{1.1}$$

Here U is a unitary matrix, called lepton mixing matrix. The matrix U can be parametrized in terms of three mixing angles $\theta_{ij} = (\theta_{12}, \theta_{23}, \theta_{13})$ and a phase factor δ,

$$U = \begin{pmatrix} c_{12}c_{13} & s_{12}c_{13} & s_{13} \\ -s_{12}c_{23} - c_{12}s_{23}s_{13}e^{i\delta} & c_{12}c_{23} - s_{12}s_{23}s_{13}e^{i\delta} & s_{23}c_{13}e^{i\delta} \\ s_{12}s_{23} - c_{12}c_{23}s_{13}e^{-i\delta} & -c_{12}s_{23} - s_{12}c_{23}s_{13}e^{-i\delta} & c_{23}c_{13} \end{pmatrix}, \tag{1.2}$$

where $c_{ij} = \cos\theta_{ij}$ and $s_{ij} = \sin\theta_{ij}$. This matrix is called the Maki-Nakagawa-Sakata (MNS) matrix [3]. The phase factor δ is due to a possible CP-violation. If neutrinos are Majorana particles, there are two additional phase factors and the mixing matrix U is multiplied by a diagonal phase matrix $diag(e^{i\eta_1}, e^{i\eta_2}, 1)$ [4]. In this thesis CP conservation is assumed, thus $\delta = \eta_1 = \eta_2 = 0$. Matrix U is build up as a product of three rotation matrix in subplanes of 3-dimensional space the θ_{ij} being associated with the rotation in the ij coordinate plane.

Neutrino phenomenology implies that neutrino mass spectrum is formed by a relatively close states ν_1 and ν_2, whose mixing explains the solar neutrino data, and a third state ν_3, which might be either heavier (normal hierarchy) or lighter (inverted hierarchy) than the ν_1,

ν_2 pair, so as to explain the atmospheric neutrinos data (see Fig. 1.1). In the ν_1, ν_2 pair the heaviest state is labeled as ν_2. In this work we will assume normal hierarchy unless where otherwise stated. The neutrino oscillation phenomena do not give direct information on the absolute scale of neutrino masses, only on mass differences. Nevertheless, the atmospheric neutrino data, which is explained by neutrino oscillations corresponding to the squared mass difference $\Delta m^2 = 2.6 \cdot 10^{-3}$ eV^2, indicate that at least one of neutrinos is heavier than 0.05 eV. The most stringent upper limit for the neutrino masses is obtained from the tritium β-decay [5, 6], which gives the upper limit 2.3 eV for the effective electron neutrino mass [7].

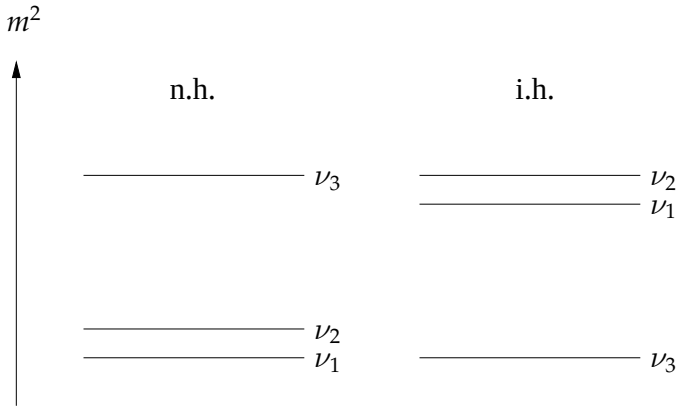

Figure 1.1: Neutrino mass spectrum in normal hierarchy (n.h.) and in inverted hierarchy (i.h.).

The ranges of mixing angles and mass-squared differences given by recent global fit analysis including data from all relevant experiments are summarized in Table 1.1.

Observation	Mixing angle	Δm^2 (eV^2)
Sun, KamLAND	$\theta_{12} = 32.4^\circ - 38.0^\circ$	$\Delta m^2_{12} = (7.01 - 9.00) \cdot 10^{-5}$
Atmosphere, K2K, MINOS	$\theta_{23} = 39.5^\circ - 53.1^\circ$	$\lvert\Delta m^2_{32}\rvert = (2.0 - 3.2) \cdot 10^{-3}$
CHOOZ	$\theta_{13} < 11.5^\circ$	$\Delta m^2_{31} \approx \Delta m^2_{32}$

Table 1.1: Neutrino mixing parameters from a global analysis of all experiments at 3σ-level [8].

1.1.2 Neutrino oscillations in vacuum

Let us consider a case of any number of neutrinos. In a plane wave approximation the evolution of neutrino weak eigenstate ν_l is given by

$$|\nu_l(t)\rangle = \sum_j e^{-iE_j t} U^*_{lj} |\nu_j\rangle, \tag{1.3}$$

where E_j is the energy of the eigenstate $|\nu_j\rangle$. At the relativistic limit $|p_j| \gg m_j$

$$E_j = \sqrt{p_j^2 + m_j^2} \simeq p_j \left(1 + \frac{m_j^2}{2p_j^2}\right) + O(m_j^4). \tag{1.4}$$

After an approximation $p_j \simeq p_i \equiv p \simeq E$ this leads to

$$|\nu_l(t)\rangle = \sum_{j,l'} e^{-i\frac{m_j^2 t}{2E}} U^*_{jl} U_{jl'} |\nu_{l'}\rangle, \tag{1.5}$$

where we have used (1.1) and dropped the unphysical overall phase p. This gives the flavor content of the neutrino state at a given time t, the state being $|\nu_l\rangle$ at $t = 0$. The amplitude for the transition $\nu_l \to \nu_{l'}$ is given as an inner product $\langle \nu_{l'} | \nu_l(t) \rangle$ leading to the probability

$$P(l \to l', L) = \sum_i |U^*_{jl}|^2 |U_{jl'}|^2 + Re\left\{ \sum_{i \neq j} U^*_{li} U_{l'i} U_{lj} U^*_{l'j} e^{-i\frac{\Delta m^2_{ij}}{2E} L} \right\}, \tag{1.6}$$

where L is the distance between production and detection points ($t \simeq L$). There is an oscillating term associated with each pair of mass eigenstates ν_i, ν_j, provided that $\Delta m^2_{ij} \neq 0$ and nonzero mixing $U_{li}, U_{l'i} \neq 0$. The oscillation length is given by

$$L_0 = \frac{4\pi E}{\Delta m^2_{ij}} = 2.48 \frac{E/\mathrm{MeV}}{\Delta m^2_{ij}/\mathrm{eV}^2} \mathrm{m}. \tag{1.7}$$

To be sensitive to the oscillations the set-up of an experiment should be such that $L \sim L_0$. If $L \ll L_0$ the oscillation phase does not have time to develop and to give an observable effect. In the case of $L \gg L_0$ the oscillation phase goes through several cycles before detection and the oscillations average out because of the spread in energy of any actual neutrino beam.

When studying neutrino oscillation phenomena, it is in many cases enough to consider a two neutrino case. The mixing matrix is then

$$U = \begin{pmatrix} \cos\theta & \sin\theta \\ -\sin\theta & \cos\theta \end{pmatrix}, \tag{1.8}$$

and the oscillation probability is given by

$$P(l \to l', L) = \sin^2 2\theta \sin^2 \frac{\Delta m^2 L}{4E}. \tag{1.9}$$

The first evidence of neutrino oscillation came from the Super-Kamiokande experiment measuring neutrinos produced in the Earth's atmosphere by cosmic rays [9]. Signals of oscillations have also been seen in solar neutrino experiments, where the observed deficit of the electron neutrinos has got a convincing explanation in terms of oscillations between the all three neutrino flavors [10]. The KamLAND reactor neutrino experiment, in which the deficit of electron antineutrino flux produced by nuclear power plants is measured, has given a clear evidence of oscillations as well [11]. Oscillation signal has also been seen in long baseline accelerator experiments K2K [12] and MINOS [13]. In future, neutrino oscillations are expected to be seen in measurements of ultra high energy cosmic ray (UHECR) neutrinos produced in distant astrophysical sources. A set of values for which atmospheric, solar, KamLAND, long baseline (LBL) and UHECR would give an oscillation signal are listed in Table 1.2.

Source	L	E	Δm^2 (eV^2)
Atmosphere	$(10^4 - 10^7)$ m	$(0.1 - 10)$ GeV	$10^{-5} - 1$
Sun	10^{11} m	$(0.1 - 10)$ MeV	$10^{-12} - 10^{-10}$
KamLAND	$150 - 210$ km	$\sim$ MeV	$\gtrsim 10^{-5}$
LBL	~ 100 km	$\sim$ GeV	$> 10^{-3}$
UHECR	~ 100 Mpc	$> 10^4$ GeV	$\geq 10^{-18}$

Table 1.2: Characteristic values of the key parameters in various neutrino oscillation experiments.

Equation of motion for weak eigenstates

The time evolution of neutrino mass eigenstates can be described by the Schrödinger equation

$$i\frac{d}{dt}|\nu_m\rangle = H|\nu_m\rangle = \begin{pmatrix} E_1 & 0 \\ 0 & E_2 \end{pmatrix} |\nu_m\rangle. \tag{1.10}$$

Here $|\nu_m\rangle$ represents a quantum mechanical neutrino state in mass basis. For relativistic neutrinos (1.4) holds, and neglecting the unimportant common phase one gets

$$i\frac{d}{dt}|\nu_m\rangle = \frac{1}{2E}\begin{pmatrix} m_1^2 & 0 \\ 0 & m_2^2 \end{pmatrix} |\nu_m\rangle = \frac{1}{2E} M_m^2 |\nu_m\rangle. \tag{1.11}$$

Using the definition of weak eigenstates $|\nu_W\rangle = U^\dagger|\nu_m\rangle$ leads to the following equation of motion

$$i\frac{d}{dt}|\nu_W\rangle = \frac{1}{2E}UM_m^2U^\dagger|\nu_W\rangle = H_0|\nu_W\rangle \tag{1.12}$$

This description is useful when considering evolution of neutrino states in matter.

1.2 Neutrinos in matter

When neutrinos travel in matter they interact with the particles of the medium, scattering on them either coherently or incoherently. At low energies only the the elastic forward scattering is relevant and inelastic scattering can be neglected. Coherence of the wave function gives rise to additional potential energy, $V_e = V_C + V_N$, where V_C and V_N denote for charged-current (CC) and neutral-current (NC) interactions, respectively [14]. In ordinary matter μ or τ leptons are not present, so that the CC reactions occur only for electron (anti)neutrinos, whereas the NC interactions happen for all flavors. The potential energies are given as [14]

$$\begin{aligned} V_C &= \pm\sqrt{2}G_F N_e, \\ V_N &= \mp\tfrac{1}{\sqrt{2}}G_F N_n, \end{aligned} \tag{1.13}$$

where upper (lower) sign refer to ν ($\bar{\nu}$), G_F is the Fermi coupling constant, and N_e (N_n) is the background electron (neutron) number density. The presence of matter changes the Hamiltonian H_0 of Eq. (1.12) to the form

$$H_m = H_0 + V = \frac{1}{2E}UM_m^2U^\dagger + \begin{pmatrix} \sqrt{2}G_F N_e & 0 \\ 0 & 0 \end{pmatrix}. \tag{1.14}$$

The term V_N, common for all flavors, is subtracted here, and an assumption $N_e = N_n$, valid in an environment with light elements, like in the Sun, is made. V is a diagonal matrix in flavor basis whose elements are the effective potentials describing the coherent forward scattering in matter (for antineutrinos $V \to -V$). Diagonalization of the Hamiltonian (1.14) gives the neutrino eigenstates in matter.

In a non-uniform medium, the Hamiltonian (1.14) and consequently its eigenstates vary as a function of electron density. In some special cases the new eigenstates can be found analytically [15], but in general the Schrödinger equation can be solved only numerically. In a medium with varying density the mixing of states can be anything quite independently of their mixing in vacuum. For a two neutrino system the effective mixing angle θ_m, i.e. the

angle that diagonalizes (1.14), is given by

$$\tan 2\theta_m = \frac{\tan 2\theta}{1 - V(r)/V_R}, \tag{1.15}$$

where $V_R = \Delta m^2 \cos 2\theta / 2E$ [4]. The point where $V(r) = V_R$ is called the resonance point. There the change of the eigenstates is most rapid and the states are maximally mixed, i.e. $\theta_m = \pi/4$. When the density grows beyond its value at the resonance, the effective mixing angle approaches gradually the value $\theta_m = \pi/2$. The smaller the vacuum mixing angle θ, the sharper is the change of the eigenstates at the resonance. The resonance condition $V(r) = V_R$ determines the resonance density to be

$$\rho^R \sim 1.4 \cdot 10^6 \frac{\mathrm{g}}{\mathrm{cm}^3} \left(\frac{\Delta m^2}{1\mathrm{eV}^2}\right) \left(\frac{10\mathrm{MeV}}{E}\right) \left(\frac{0.5}{Y_e} \cos 2\theta\right), \tag{1.16}$$

where Y_e is the electron fraction in the medium, defined as the number of electrons per nucleon. One can define the resonance width $\Delta\rho^R$ as the distance from ρ^R where $\sin^2 2\theta$ becomes half of its maximum value. For a small vacuum mixing angle θ, the width of the resonance layer is [16]

$$2\Delta\rho^R \approx 2\rho^R \tan 2\theta. \tag{1.17}$$

The layer where the density changes in the interval $\rho^R \pm \Delta\rho^R$ is called the resonance region.

1.2.1 The MSW effect

Let us consider the evolution of a neutrino state before and after a resonance more carefully. The behavior of the eigenstates of a two-neutrino system in medium with varying density is illustrated in Fig. 1.2, where the effective mass squared m^2_{eff}, obtained by diagonalizing (1.14), is plotted as a function of $A = 2EV$. For large values of A, i.e. in dense matter, the angle θ_m approaches asymptotically the value $\pi/2$, the faster the smaller the vacuum mixing angle θ. Hence at the production point, e.g. in a dense core of a supernova, the electron neutrino ν_e is more or less the pure ν_2. The state ν_2 propagates in medium with decreasing density feeling no much oscillation until the resonance region is reached. There oscillation enhances, and neutrino becomes half ν_e and half ν_a (ν_μ or ν_τ), since θ_m becomes $\pi/4$ regardless of the value of the vacuum mixing angle, as indicated by Eq. (1.15). As neutrino leaves the resonance region the ν_a component increases and the neutrino enters the vacuum as the mass eigenstate ν_2. This behavior of the neutrino system is known as Mikheyev-Smirnov-Wolfenstein (MSW) effect [14, 17]. This description is valid when many oscillations take place at the resonance

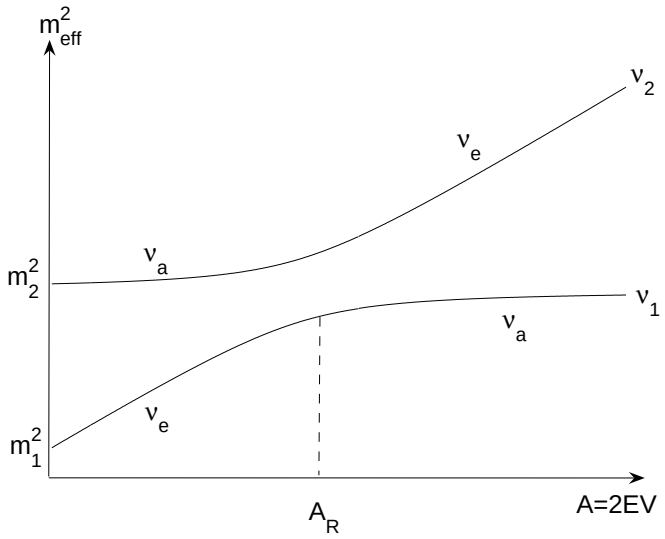

Figure 1.2: The MSW effect. ν_e produced in high density follows the ν_2 curve. In resonance the mixing is maximal and the neutrino continues as ν_2. It ends up to vacuum as ν_a.

region and the system has time to adjust itself. Such transition is called adiabatic. If the oscillation length is of the same order or greater than the width of resonance layer, the system does not behave adiabatically. Then a transition will take place from state ν_2 to state ν_1 in the resonance layer. The probability of this level crossing was first derived by Landau and Zener [18, 19]. The Landau-Zener model for level crossing will be discussed in detail in Chapter 3.

1.3 Sterile neutrinos

All the original research articles of this thesis concern sterile neutrinos. A sterile neutrino is a singlet under the SM gauge interactions, i.e. it is assigned into the representation $(\mathbf{1}, 0)$ under the SM gauge symmetry $SU(2)_L \times U(1)_Y$. In the most simple scenario it is identified as a right-handed neutrino. The existence of sterile neutrinos is predicted by many extensions of SM [20]. Often the new fermions are not called neutrinos, though transforming as $(\mathbf{1}, 0)$, since they may originate from different physics. A singlet fermion may be a mirror neutrino, goldstino in SUSY, modulino of the superstring theories or a bulk fermion related to the existence of extra dimensions.

Let us first consider the case where sterile neutrinos are identified with right-handed neutrinos, which are introduced in most models of neutrino mass. Right-handed neutrinos

have to be introduced, if one wants to have Dirac mass terms $\bar{\nu}_R \nu_L + h.c.$ in the theory [21]. Actually, symmetry arguments seem to imply that there is one sterile neutrino per fermion family. A left-right symmetry of the matter content of particle theory would require that each left-handed fermion has a right-handed counterpart. In the SM, neutrinos are the only exception to this symmetry. A lepton-quark symmetry would imply that for each quark with a given chirality there exists a lepton counterpart. The absence of right-handed neutrinos would violate this symmetry.

The most general mass term for a single neutrino flavor is

$$\mathcal{L}_{\mathcal{M}_\nu} = -\frac{1}{2}\overline{\nu^c}\mathcal{M}\nu + h.c., \tag{1.18}$$

where $\nu = (\nu_L \nu_R^c)^T$, $\nu_{L,R}$ denoting left-handed and right-handed fields and ν^c the charged conjugated field, and $\mathcal{M}$ is a symmetric complex matrix

$$\mathcal{M} = \begin{pmatrix} m_L & m_D \\ m_D & m_R \end{pmatrix}, \tag{1.19}$$

where m_D and $m_{L,R}$ are the Dirac and Majorana masses, respectively. The Dirac mass term m_D originates from the Yukawa couplings of the neutrino to the Higgs doublet ϕ, similarly as the mass terms of charged leptons, and it is thus proportional to the electroweak symmetry breaking scale. The Majorana mass term for the left-handed neutrinos is $m_L\overline{(\nu^c)_R}\nu_L + h.c.$ It can arise through spontaneous symmetry breaking from a coupling of the neutrino with an $SU(2)_L$ triplet Higgs field or from a non-renormalizable coupling with the product $\phi\phi$. The Majorana mass term for the right-handed neutrino, $m_R\overline{(\nu^c)_L}\nu_R + h.c.$, is $SU(2)_L \times U(1)_Y$ invariant and it can appear as a bare mass term in the Lagrangian. None of these mass terms are present in the SM as there is no right-handed neutrino in the model (as it would not have any gauge interactions) and lepton number violating terms will not arise in perturbation theory as the all couplings of the model are lepton number conserving. If $m_{L,R} = 0$ neutrinos are Dirac particles, while for nonzero values of $m_{L,R}$ they are Majorana particles, independently of the value of m_D.

A couple of special mass scenarios are of particular interest. One of them is the seesaw model [22, 23, 24], which predicts the existence of heavy sterile neutrinos. In the seesaw case an assumption $m_R \gg m_D \gg m_L \simeq 0$ is made as m_R is assumed to associate with a Grand Unified Scale 10^{16} GeV or with some other high energy scale, m_D is associated with the electroweak scale 10^2 GeV, and m_L is small compared with m_D since a large vacuum expectation value of a triplet Higgs field would be in contradiction with the measured mass ratio of W

and Z bosons. In this case the mass eigenvalues become $m_1 \simeq m_D^2/m_R$ and $m_2 \simeq m_R$ [4]. The two masses differ enormously, the heavier state being predominantly sterile. The smaller eigenvalue $m_1 \ll m_D$, explaining why the ordinary neutrinos are much lighter than other fermions. The seesaw mechanism is the most popular explanation for the smallness of neutrino mass. It also predicts the mixing between active and sterile states to be very small ($\tan 2\theta = 2m_D/(m_R - m_L)$), which could explain why the light sterile states, if they exist, have been effectively hidden from the current low-energy neutrino phenomenology.

The seesaw mechanism is not, however, the only way to generate neutrino mass hierarchy. It is quite possible that light sterile neutrinos exist. They would appear, for example, if the Dirac mass dominates over the Majorana masses in the mass matrix (1.19) $m_L, m_R \ll m_D$. This would lead to mass eigenvalues $m_{1,2} \simeq m_D \pm m_R/2$ and a mixing angle $\tan 2\theta = -2m_D/m_R \Rightarrow |\theta| \simeq \pi/4$. This is called the pseudo-Dirac model, because in the limit where Majorana mass term approaches zero the two neutrinos are combined and they form a Dirac particle. Pseudo-Dirac neutrinos are nearly degenerate in mass and have a nearly maximal active-sterile mixing. A drawback of the pseudo-Dirac model is that it does not offer any immediate explanation for the smallness of m_D in comparison with the other Dirac masses of SM. A number of suggestions has been made to cure this. For example, Dirac masses could be small because they might be forbidden in a tree-level and arise only through radiative corrections as a result of a Dirac seesaw mechanism [25] or they might appear as a result of different spread of neutrino and charged lepton wave functions in extra dimensions [26].

The mirror model [27] can produce a similar mass spectrum as one has in the pseudo-Dirac case. The mirror particles were introduced originally in order to maintain in a wide sense the left-right symmetry of the world broken by the parity violation of weak interactions [28, 29]. Mirror world originates from space inversion which in addition to parity transformation transforms a particle into a reflected state in the mirror particle space [30]. Mirror particles have interactions identical to the ordinary particles, except with the opposite chirality. They are assumed to interact with the ordinary particles only gravitationally or via Higgs potential and neutrino mixing [31]. In the mirror world the weak interactions are right-handed and thus the counterparts of the ordinary active neutrinos in mirror world could be identified as sterile neutrinos. Because the analogue of the ordinary and mirror world, whatever mechanism makes the ordinary neutrinos light, the same mechanism is assumed to operate also in the mirror sector [20].

Sterile neutrinos that mix with the ordinary neutrinos might have been produced in the

early universe via oscillations and they could have had important cosmological implications. The most significant effect concerns the Big Bang Nucleosynthesis, which successfully explains the abundances of light elements [32]. BBN constrains the number of relativistic particle species in thermal equilibrium and the neutrino contribution to the critical density of the universe. Sterile neutrinos could contradict with these constraints unless the mass-squared differences and/or the active-sterile mixing angles are small enough [33, 34, 35, 36, 37]. For the $\nu_e \leftrightarrow \nu_s$ mixing a bound $|\Delta m^2| \sin^2 2\theta < 5 \times 10^{-8}\ \mathrm{eV}^2$ has been obtained, while for the $\nu_{\mu,\tau} \leftrightarrow \nu_s$ mixing the bound is $|\Delta m^2| \sin^2 2\theta < 7 \times 10^{-5}\ \mathrm{eV}^2$ [38].

So far the existence of sterile neutrinos has been neither confirmed nor ruled out. Measurements of solar, atmospheric, reactor and beam neutrinos have restricted the allowed range in parameter space for sterile neutrinos. Previously the positive $\bar{\nu}_\mu \rightarrow \bar{\nu}_e$ oscillation signal from LSND experiment [39] sensitive to the mass scale $\Delta m^2 \sim 1\mathrm{eV}^2$ was explained by a existence of a sterile neutrino [40]. Recently, the interpretation of this result in terms of a single sterile neutrino has become strongly disfavored due to the first results of the MiniBooNE experiment [41], where no indication of neutrino oscillation has been seen . But there is still plenty of free parameter space for sterile neutrinos left [42].

Because sterile neutrinos lack gauge interactions, they can not be produced or detected in weak interaction processes. When mixing with active neutrinos, sterile neutrinos might be formed via oscillation or matter effects. In this thesis the former have been studied in Paper I in the case of UHECR neutrinos, the latter in Papers II-IV in the case of supernova neutrinos. It is shown in these papers that the existence of a sterile state can be deduced via deficit of the flux of active neutrinos.

Chapter 2

Neutrinos from astrophysical sources

In this Chapter we first shortly review the solar neutrino problem and the results from various solar neutrino experiments. Then we introduce the distant astrophysical neutrino sources relevant to this work, supernovae and sources of ultrahigh-energy neutrinos.

2.1 Solar neutrinos

One of the most significant experimental achievements in neutrino physics is the observation of neutrinos from the Sun. Solar energy is produced via nuclear fusion reactions, where protons are converted into alpha particles, positrons and neutrinos. According to the Standard Solar Model (SSM), there are eight nuclear reactions which produce neutrinos [43]. Five of them belong to the so-called pp cycle, and neutrinos produced in these reactions are called the pp, ^8B, hep, ^7Be and pep neutrinos, named after the source or producing reaction. The first three have continuous energy spectrum, while the last two are monoenergetic. The ^{13}N, ^{15}O and ^{17}F neutrinos originate from the so-called CNO cycle and have continuous spectrum. We will concentrate on the dominant pp chain. The fluxes of the pp chain neutrinos predicted by SSM are shown in Fig. 2.1, where the detection regions of different experiments are also indicated.

The pioneering experiment detecting solar neutrinos was the Homestake experiment [45]. It is known also as a chlorine experiment, because the detection of neutrinos is based on the radiochemical reaction $\nu_e + {}^{37}Cl \rightarrow {}^{37}Ar + e^-$. The energy threshold for this reaction is 0.814 MeV. According to Fig. 2.1 the Homestake experiment is sensitive to the ^8B and ^7Be neutrinos. Another class of radiochemical experiments are the so-called Gallium experiments

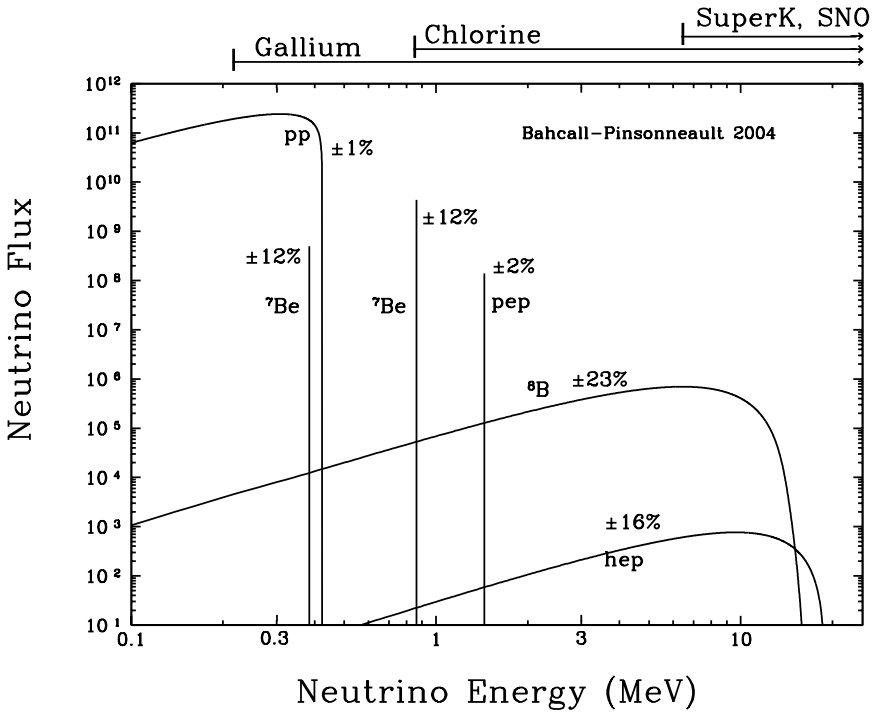

Figure 2.1: Solar neutrino energy spectrum for pp chain predicted by BP04 [44]. Total theoretical uncertainties are shown for each source. Thresholds of various solar neutrino experiments are shown at the top.

SAGE [46], GALLEX [47] and GNO [48]. They detect solar neutrinos via reaction $\nu_e + {}^{71}Ga \rightarrow {}^{71}Ge + e^-$ with a low threshold of 0.233 MeV. Therefore they are sensitive also to the pp neutrinos.

The real time measurement of the solar neutrinos is possible by using water Čerenkov detectors. They capture the Čerenkov light emitted by the electrons created by the elastic scattering reaction $\nu_x + e^- \rightarrow \nu_x + e^-$. The first experiments based on this method were the Kamiokande experiment [49] and its successor Super-Kamiokande experiment [50]. Unlike radiochemical experiments, the Čerenkov light experiments are sensitive to all neutrino flavors because the elastic scattering of neutrinos on electron can happen via both charge current (CC) and neutral current (NC) reactions. The cross section of the ν_μ and ν_τ (NC) scattering is about six times smaller than that of the ν_e scattering (CC and NC). The energy threshold of the Kamiokande experiment was 7.5 MeV while at the Super-Kamiokande experiment it

was 5 MeV, which means that both experiments can measure only the ^8B neutrinos (the contribution of *hep* neutrinos is negligible).

The most advanced solar neutrino experiment is the SNO experiment [10], which proved that part of the electron neutrinos transform to muon and tau neutrinos on their way from the core of the Sun to the Earth. The target material in the SNO experiment is heavy water, D_2O. The significance of the SNO results follows from the possibility to detect neutrinos via three different channels:

1. Neutral Current (NC): $\nu_x + d \rightarrow n + p + \nu_x$
2. Charged Current (CC): $\nu_e + d \rightarrow p + p + e^-$
3. Elastic Scattering (ES): $\nu_x + e^- \rightarrow \nu_x + e^-$

The CC reaction is sensitive only to ν_e, while NC and ES reactions are sensitive to all neutrino flavors. The NC reaction has equal cross section for all flavors but the ES reaction has six times larger cross section for the electronic than for the other flavors. The CC and ES reactions have a threshold of 5 MeV and that of the NC reaction is 2.2 MeV. Hence these reactions are sensitive only to the ^8B neutrinos.

The solar neutrino problem consists of the apparent deficit of electron neutrinos arriving on Earth compared with the flux predicted by the SSM. The deficit is seen in all above mentioned experiments, in which $30-52\%$ of the theoretical flux has been detected [8]. The exact fluxes versus the theoretical predictions for the various experiments are presented in Fig. 2.2. The last two pair of bars in Fig. 2.2 are due to SNO experiment. In concord with the previous results, the SNO measured in the CC channel about one third of the predicted flux, while the NC flux coincides with the theoretical prediction for the total production of neutrinos in the Sun.

The SNO results confirmed that neutrinos do change flavor, indicating that they are massive particles and that they mix. A combined analysis of solar neutrino data and the data of the KamLAND reactor neutrino experiment [11] gives the best-fit values $\Delta m^2_{12} = 8.2 \cdot 10^{-5}\,\mathrm{eV}^2$ and $\theta_{12} = 31^\circ$ [53] for the $\nu_e \rightarrow \nu_{\mu,\tau}$ oscillation parameters. This is called the Large Mixing Angle (LMA) solution. The recent results from Borexino experiment [54] measuring mainly ^7Be neutrinos are also consistent with the predictions of the LMA solution.

The resonance density depends on the neutrino energy according to (1.16). In the LMA, high energy solar neutrinos undergo MSW effect described in section 1.2.1, as the resonance density is much lower than the density at the neutrino production point. Instead, at low

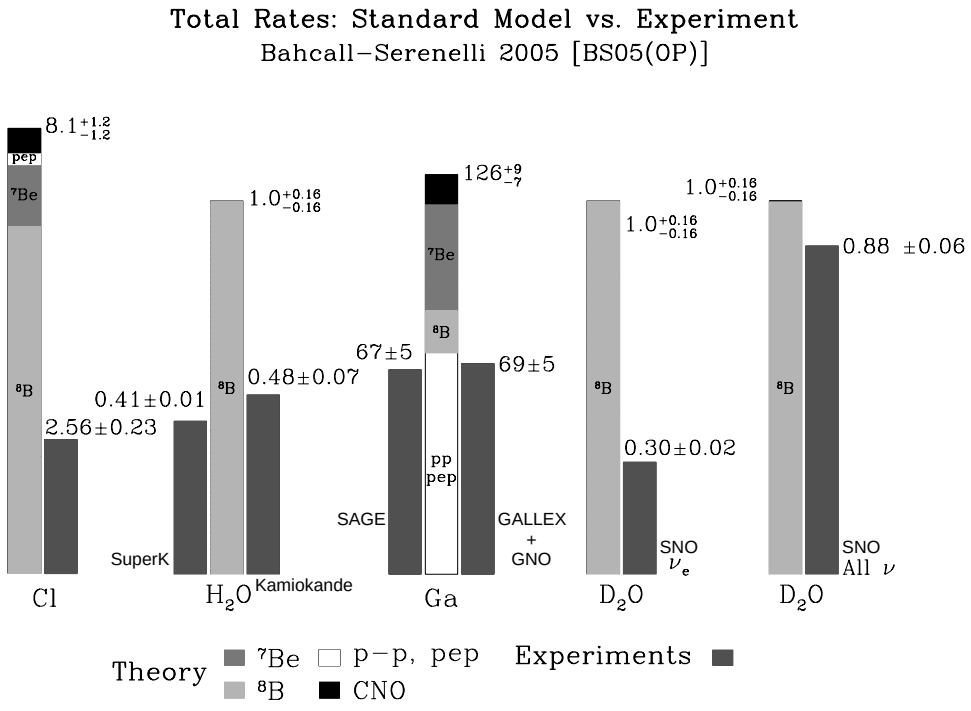

Figure 2.2: Theory versus experiments [51]. The figure compares the predictions of the standard models of the Sun [52] and electroweak interactions to the measured rates in Solar neutrino experiments.

energies the resonance density exceeds the density of the production point. Therefore low energy solar neutrinos experience vacuum oscillations [55]. Because the SNO experiment is sensitive only to ^8B neutrinos, there is still plenty of unexplored space in the low energy part of the spectrum to be studied in future experiments like CLEAN [56], which will have a energy threshold of $\lesssim 20$ keV.

2.2 UHECR neutrinos

In distant astrophysical objects like active galactic nuclei (AGN) and gamma ray bursts (GRBs) ultrahigh-energy neutrinos ($E \geq 10^6$ GeV) are thought to be produced. AGN are bright and compact central regions of galaxies. It is hypothesized that in AGN a supermassive black hole accretes matter, causing emission of highly powered jets of matter that stream out of the

central region. The origin of GRBs is more unclear, a fireball model has been suggested [57]. In addition to AGN and GRBs, ultrahigh-energy neutrinos may also be produced in so-called top-down sources, where neutrinos are produced in decays and annihilation of heavy particles [58]. Examples of such sources are topological defects, monopoles and cosmic strings, and decays of massive relic particles originating from string and supergravity theories [59].

It is supposed that in AGN and GRBs hadrons are accelerated to very high energies. Collisions like $p\gamma$ and pp will occur, yielding pion production and decays and subsequent muon decays:

$$\begin{aligned} \pi &\rightarrow \mu + \nu_\mu \\ &\quad\ \downarrow \\ &\quad\ \mu \rightarrow e + \nu_e + \nu_\mu, \end{aligned} \tag{2.1}$$

with nearly equal amount of particles and antiparticles. The initial neutrino fluxes from the source are thus related as $F_e^0 : F_\mu^0 : F_\tau^0 = 1 : 2 : 0$, where F_e^0, F_μ^0 and F_τ^0 are the initial fluxes of electron, muon and tau neutrinos, respectively. Because the distance of UHECR neutrino production point from the Earth and the energy of produced neutrinos vary, the oscillations will average out in the data. Thus the time dependence of the survival probability (1.6) disappears and the probability is given by

$$P(l \rightarrow l') = \sum_j |U_{jl}|^2 |U_{jl'}|^2. \tag{2.2}$$

Assuming no significant matter effects on the route, the observed flux of each flavor ν_l on the Earth is

$$F_l = \sum_{l'} P(l' \rightarrow l) \cdot F_{l'}^0. \tag{2.3}$$

If no new physics is present the fluxes of different neutrino flavors measured at the Earth should be roughly equal. This can be understood as follows. The initial fluxes in the mass basis are $F_i^0 = \sum_l |U_{li}|^2 F_l^0$. Using the information that $|U_{e3}| \simeq 0$ and that atmospheric mixing is nearly maximal one gets $F_1^0 : F_2^0 : F_3^0 \approx 1 : 1 : 1$ irrespective of the solar angle θ_{12} (see e.g. [60, 61, 62]). Oscillations do not change these proportions but only the relative phases between the mass eigenstates. An incoherent mixture in the ratios $F_1 : F_2 : F_3 \approx 1 : 1 : 1$ in the mass basis leads to equal mixture also in flavor basis, i.e. $F_e : F_\mu : F_\tau \approx 1 : 1 : 1$.

The detection of UHECR neutrinos will be a challenge due to the low fluxes and a substantial background of atmospheric neutrinos [63]. One of the most appropriate techniques for detecting UHECR neutrinos consists of detecting Čerenkov light from muons or showers produced by neutrino interactions in large volume underground water or ice telescopes

like IceCube [64], ANTARES [65] and NESTOR [66]. Neutrino fluxes from individual AGN or GRB are not detectable, but the diffuse flux might be detected in the future experiments mentioned above.

Deviations from the equal flux prediction in future experiments would be an indication of new physics. The deviation might be due to non-conventional production mechanism [67], neutrino decay [68] or CPT violation [69]. It may give a hint that neutrinos are pseudo-Dirac particles [70]. It can also indicate a presence of sterile neutrinos [61], whose effects have been studied in this thesis in Paper I.

2.3 Supernova neutrinos

Supernovae of type II are thought to be originated by core collapses of red or blue giant stars with mass $M \geq 8M_\odot$, where $M_\odot$ is the mass of the Sun. Since the remnant of the collapsed star and the surrounding envelope are optically thick, most of the gravitational binding energy ($\sim 10^{53}$ ergs) is carried away by neutrinos. Their average energy is 10 MeV, and their number is about 10^{58} [71].

Rate estimates of core collapse supernovae in the Milky Way vary somewhat, typical value being a few in a century. In 1987 a supernova explosion took place in the Large Magellanic Cloud, which is 51.8 kpc away from the Earth. About 20 neutrinos from this explosion, known as SN1987A, were detected in the Kamioka [72] and IMB [73] experiments. Any far-going conclusions could not have been made from the data because of poor statistics. In two decades the number of detectors has increased and the quality of resolution have improved such a way that thousands of events would be detected from a supernova explosion taking place in our galaxy today.

Supernova explosion takes place when the iron core of a massive star reaches the so-called Chandrasekhar limit of about $1.4M_\odot$ [4]. In the hot core neutrinos of all flavors are produced. Electron (anti)neutrinos are dominantly produced in the CC processes like $e^- + p \rightarrow n + \nu_e$ and $e^+ + n \rightarrow p + \bar{\nu}_e$, while other flavors are produced in several different NC processes such as electron-positron pair annihilation $e^+ + e^- \rightarrow \nu_l + \bar{\nu}_l$, electron-nucleon bremsstrahlung $e^\pm + N \rightarrow e^\pm + \nu_l + \bar{\nu}_l$, and nucleon-nucleon bremsstrahlung $n + p \rightarrow n + p + \nu_l + \bar{\nu}_l$ [71].

In spite of the weakness of their interactions, neutrinos are trapped in the core because of the very high matter density. They can freestream only when the density is low enough so that the neutrino mean free path is larger than the radius of the core. The surface from which neutrinos freestream is called neutrinosphere and its radius depends on the flavor and

energy of neutrinos. Since ν_μ, $\bar{\nu}_\mu$, ν_τ and $\bar{\nu}_\tau$ (called collectively ν_x in the following) feel only the NC interactions, they leave the local thermal equilibrium earliest and have the smallest radii of neutrinosphere. Since the mantle is neutron-rich, the reaction $\nu_e + n \rightarrow e^- + p$ is more efficient than $\bar{\nu}_e + p \rightarrow e^+ + n$. This keeps ν_e in local thermal equilibrium up to larger radii than $\bar{\nu}_e$. Thus the next deepest neutrinosphere is that of $\bar{\nu}_e$ and the least deep one is that of ν_e. The estimated radii of the neutrinospheres lie between about $50 - 100$ km [71]. The larger the radius of the neutrinosphere, the lower the mean energy of neutrinos. Based on that, the hierarchy of average energies is supposed to be

$$\langle E_{\nu_e} \rangle < \langle E_{\bar{\nu}_e} \rangle < \langle E_{\nu_x} \rangle. \tag{2.4}$$

There is an uncertainty considering the initial spectrum of supernova neutrinos. The above assumptions lead to the traditional prediction of roughly equal initial fluxes $F_e^0 : F_{\bar{e}}^0 : F_x^0 = 1 : 1 : 1$ [74]. In Ref. [75] the nucleon recoils and electron neutrino pair annihilation $\nu_e + \bar{\nu}_e \rightarrow \nu_l + \bar{\nu}_l$ have been included in the simulation and spectrum presented in Fig. 2.3 for neutrino fluxes has been obtained. As can be seen from Fig. 2.3, for the average energies it implies $\langle E_{\bar{\nu}_e} \rangle \approx \langle E_{\nu_x} \rangle$, in contrast to (2.4). Neutrino number fluxes can still differ by a large amount. When integrated over the energy the neutrino flux ratios $F_e^0 : F_{\bar{e}}^0 : F_x^0 = 4 : 3 : 2$ are obtained.

The effective potential met by neutrinos in a supernova is proportional to the matter density of the progenitor star. According to [76] the effective potential felt by ν_e is described by the radial power-law

$$V(r) = 1.5 \cdot 10^{-9}\ \mathrm{eV} \left(\frac{10^9 \mathrm{cm}}{\mathrm{r}} \right)^3. \tag{2.5}$$

In the outer layers of the envelope the density drops faster than (2.5) suggests, becoming closer to an exponential decrease [77]. However, the resonance transition at lower densities does not significantly depend on the details of the profile of the supernova [78].

According to the current knowledge of neutrino mass and mixing parameters, neutrinos undergo two MSW resonances when they traverse the star. They are denoted as H- and L-resonances, corresponding to high and low resonance density (see Fig. 2.4). The H-resonance is characterized by the mixing parameters Δm^2_{13} and θ_{13}, whereas the L-resonance corresponds to Δm^2_{12} and θ_{12}. Given the present value of Δm^2_{13} from the atmospheric and θ_{13} from the CHOOZ reactor neutrino data ($\Delta m^2_{13} = 2.6 \cdot 10^{-3}\ \mathrm{eV}^2$, $\theta_{13} < 11.5^\circ$), and those of Δm^2_{12} and θ_{12} ($\Delta m^2_{12} = 7.9 \cdot 10^{-5}\ \mathrm{eV}^2$, $\theta_{12} = 33.7^\circ$) from the solar neutrino data, as well as the average energy of supernova neutrinos, one can estimate the H- and L-resonances to occur at the

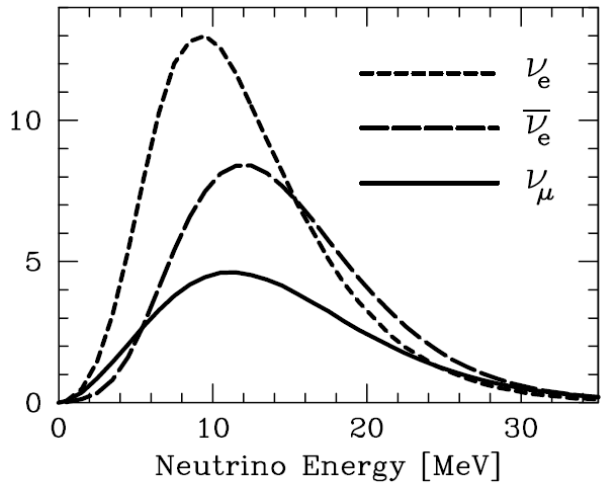

Figure 2.3: The initial spectra of neutrinos from supernovae [75]. The fluxes of $\bar{\nu}_\mu$, ν_τ and $\bar{\nu}_\tau$ are equal to that of ν_μ presented in the plot. Integration over energy gives $F_e^0 : F_{\bar{e}}^0 : F_x^0 = 4 : 3 : 2$. The ratios corresponding to the most common energy $E \sim 10$ MeV are $F_e^0 : F_{\bar{e}}^0 : F_x^0 = 4 : 2.3 : 1.4$.

densities

$$\begin{aligned} \rho_H &\approx 10^3 \text{ g} \cdot \text{cm}^{-3}, \\ \rho_L &\approx 30 - 140 \text{ g} \cdot \text{cm}^{-3}, \end{aligned} \tag{2.6}$$

respectively. The H-resonance is in the neutrino (antineutrino) channel for normal (inverted) hierarchy of neutrino masses. The L-resonance occurs for neutrinos for both the hierarchies and it is adiabatic [80]. The adiabaticity of the H-resonance depends on the value of the mixing angle θ_{13}. The adiabaticity can be calculated using the Landau-Zener formula to be discussed in detail in Chapter 3. Three cases can be distinguished [81] (P_H is the transition probability in the H-resonance):

1. Adiabaticity breaking region: $\sin^2\theta_{13} \lesssim 10^{-6} \times (E/10 \text{ MeV})^{2/3}$, where $P_\text{H} \approx 1$;
2. Transition region: $\sin^2\theta_{13} \sim (10^{-6} - 10^{-4}) \times (E/10 \text{ MeV})^{2/3}$, where $0 \lesssim P_\text{H} \lesssim 1$;
3. Adiabatic region: $\sin^2\theta_{13} \gtrsim 10^{-4} \times (E/10 \text{ MeV})^{2/3}$, where $P_\text{H} \approx 0$.

The transition region is usually neglected in analytic calculations for simplicity and the H-resonance is assumed to be either totally adiabatic or totally nonadiabatic. The sensitivity of the H-resonance on the mixing angle θ_{13} makes supernova neutrinos an excellent tool for

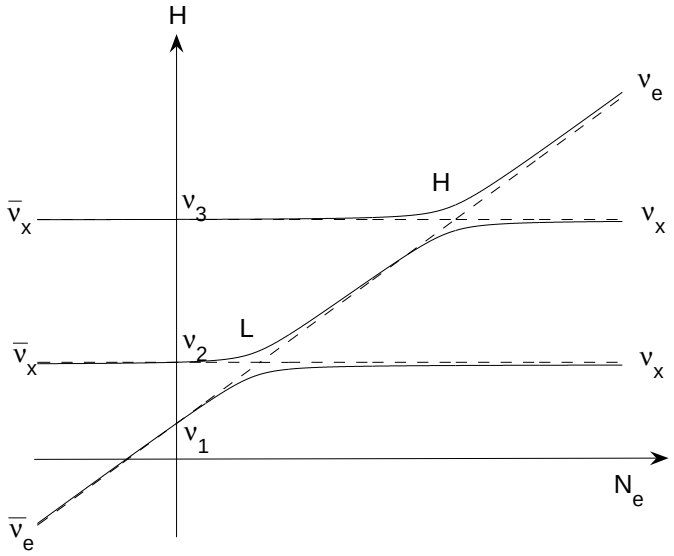

Figure 2.4: Level crossing diagram for normal mass hierarchy [79]. Solid lines show the effective Hamiltonian as a function of electron number density. The dashed lines correspond to energies of unmixed flavor levels.

studying the value of that angle. The question is especially interesting because the possible detectivity of CP-violation of neutrinos depends on the size of θ_{13}.

In the core where neutrinos are produced the density is very large ($\rho \gtrsim 10^{12}$ g $\cdot$ cm^{-3}) [82] and neutrino mixing is highly suppressed by matter effects. Because $V \gg H_0$ the Hamiltonian (1.14) is approximately diagonal and hence the interaction eigenstates coincide with the eigenstates of the Hamiltonian. If all the resonances neutrinos encounter are either adiabatic or nonadiabatic the neutrinos either stay in the original eigenstate or jump to another eigenstate completely. In such cases there is thus no mixing of eigenstates when neutrinos travel in the star and they leave the star as a single mass eigenstates and there will be no neutrino oscillations when neutrinos travel to the Earth [83]. If instead the H-resonance lies in the transition region, the behavior of the neutrino state in the resonance is semiadiabatic and a jump to another eigenstate is not complete. In that case a linear combination of eigenstates is formed and some oscillation is generated.

If neutrinos cross the Earth before detection, they may undergo matter effects in the interior of the Earth. The matter density in the Earth, $\rho \approx (1 - 13)$ g $\cdot$ cm^{-3}, is close to that of

the L-resonance. Therefore the mixing angle in matter, given by (1.15), increases from its vacuum value by the effect of the resonance, leading to oscillations which may be observable. This could affect either the flux of ν_e only or $\bar{\nu}_e$ only, or both. The Earth effect is expected to be more significant at higher energies. The energy dependence of the ν_e and $\bar{\nu}_e$ flux has an oscillatory character. The oscillatory behavior or its absence is different for detectors located differently on the Earth. It may also be possible to identify the Earth effect through the distortion of the spectrum in a single detector [84].

Chapter 3

Landau-Zener theory and its extensions

The Landau-Zener (LZ) model [18, 19] is widely used for solving the time-dependent Schrödinger equations. It is a method for evaluating the transition probabilities between two states in a linear quantum system, and it is based on the WKB approximation, where approximative solutions of Schrödinger equation are used. The method is quasi-classical, meaning that the de Broglie wavelengths are assumed to be small compared with the characteristic dimensions of the system, which holds when potential varies slowly and the momentum of the particle is nearly constant over several wavelengths.

Originally the LZ-theory was applied to transitions in diatomic molecules [18], but it has found applications also in atomic and molecular physics [85], quantum optics [86], as well as in neutrino physics [87]. The motivation to use LZ-theory in neutrino physics is that it describes transitions between neutrino eigenstates in matter. In neutrino physics one is usually considering nonlinear systems as the matter densities in the physically interesting situations are usually not varying in linear manner. Applying the LZ-method to nonlinear two-level neutrino system is studied e.g. in [88]. In other fields of physics the extension of the LZ-method to multistate linear systems has been studied [86]. In particular, it has been found that in the case of linear multilevel systems analytic solutions to LZ problem exist only in some special cases [89].

In neutrino physics with current knowledge of mixing parameters and supposing active neutrinos only, all situations can be handled as separate nonlinear two-state systems. If sterile neutrinos exist, nonlinear multistate systems might be encountered. This kind of situation is

studied in detail in Paper III of this thesis.

3.1 Level crossing problem for a two-state system

Let us consider a dynamical system consisting of two states, whose energies have different time dependence. The behavior of the system is governed by the Schrödinger equation

$$i\frac{d\Psi(t)}{dt} = H(t)\Psi(t), \tag{3.1}$$

where the Hamitonian is assumed to have the form

$$H(t) = \begin{pmatrix} H_{aa} + V_a(t) & H_{ab} \\ H_{ba} & H_{bb} + V_b(t) \end{pmatrix}, \tag{3.2}$$

where the potentials V_a and V_b are different functions of time and the time-independent elements H_{aa}, H_{bb}, H_{ab} and H_{ba} correspond to the Hamiltonian in vacuum. The nondiagonal elements H_{ab} and H_{ba} arise from the coupling of states. In the presence of potentials V_a and V_b the gap between the energy levels will be time-dependent. The width of this gap is given by the difference of the energy eigenvalues, i.e.

$$\Delta E = \sqrt{(H_{aa} + V_a(t) - H_{bb} - V_b(t))^2 + 4H_{ab}^2}. \tag{3.3}$$

The system originally in one state can tunnel quantum mechanically to the other state over this gap. By a quasi-classical method described in [90] a following formula for probability of this tunneling is obtained:

$$P_{LZ} = e^{-2\Im\int^{t_0}\Delta E dt} = \exp\left(2\Im\int^{t_0} dt\sqrt{(H_{aa} + V_a(t) - H_{bb} - V_b(t))^2 + 4H_{ab}^2}\right). \tag{3.4}$$

The integration limit t_0 is a zero of (3.3). It is called the transition point and it lies on the upper half of complex plane. Non-reality of the transition point reveals that the region is classically inaccessible. In the case of several zeros, the one lying closest to the real axis is chosen as the contribution related to the other zeros is in general exponentially suppressed in comparison with the contribution of the closest zero. For the lower limit of the integration, any point on the real axis can be chosen, because the real part of the integral does not matter in (3.4).

Whether the integral in Eq. (3.4) can be solved analytically or not, depends on the exact form of the potentials $V_a(t)$ and $V_b(t)$. In general case it cannot be solved in a closed form but a numerical evaluation is needed.

When the time-dependence of the potential is linear, i.e. $V_a = v_a t,\ V_b = v_b t$, the integral in Eq. (3.4) can be solved analytically. This is the original Landau-Zener problem. One obtains in this case the following expression for the transition probability [18]:

$$P_{LZ} = \exp\left[\frac{-2\pi H_{ab}^2}{|v_a - v_b|}\right] \equiv e^{-\frac{\pi\gamma}{2}}, \tag{3.5}$$

where an adiabaticity parameter γ has been defined:

$$\gamma = \frac{4H_{ab}^2}{|v_a - v_b|}. \tag{3.6}$$

Adiabatic conversions correspond to the values $\gamma \gg 1$ and the transition probability $P_{LZ} \simeq 0$. Then the oscillation length changes slowly compared with the potential V and the eigenstates propagate without mixing. In the case $\gamma \lesssim 1$ the transition is nonadiabatic and a level crossing from one state to another can occur. The transition probability can be calculated from classical equations of motion although the tunneling process itself is classically forbidden, as the complexity of the transition point implies, hence the term quasi-classical [90].

3.2 Parametrization for LZ problem in neutrino physics

In neutrino physics, the two-state Hamiltonian (1.14) is inserted into the generalized definition of adiabaticity parameter, where the denominator of the definition (3.6) is replaced by the absolute value of the spatial derivative of the difference of the potentials at the resonance point. The resonance condition $V_R = \Delta m^2 \cos 2\theta / 2E$ leads to the following expression for the adiabaticity parameter [87]:

$$\gamma = \frac{\Delta m^2 \sin^2 2\theta}{2E \cos 2\theta |dN_e/N_e dx|_R}. \tag{3.7}$$

Here the subscript R denotes the resonance point, corresponding to the turning point discussed in the previous section, at which the logarithmic derivative of the electron number density N_e should be evaluated.

Usually the potentials neutrinos experience when traveling in matter are nonlinear due to nonlinear density profiles of the medium. For example, in the Sun the potential is exponential, while in supernovae it is assumed to have a power-law form. The original Landau-Zener formula (3.5) is not applicable in these cases but one needs to evaluate the integral (3.4). For some special cases, like exponential and power-law potential, it turns out that the adiabaticity parameter γ factors out of the integral and an expression depending only on the mixing

angle θ (and in the case of power-law potential the power n) is left [88]. The formula (3.5) generalizes to the form

$$P_{LZ} = e^{-\frac{\pi\gamma}{2}\mathcal{F}_n(\theta)}, \tag{3.8}$$

where $\mathcal{F}_n(\theta)$ is the correction function that takes into account the nonlinearity of the potential V. The parameter γ can still be approximated as in Eq. (3.7). The proper definition of γ in nonlinear case would contain higher order derivatives. Nevertheless, it is enough to include the first order derivative, the rest is taken into account by the correction function $\mathcal{F}_n(\theta)$ [88].

According to Ref. [88], the correction function for an exponential potential ($V \propto \exp(-r)$) experienced by neutrinos traveling in the Sun is

$$\mathcal{F}(\theta) = 1 - \tan^2\theta, \tag{3.9}$$

and for a power-law potential ($V \propto r^n$) experienced in supernovae it is

$$\mathcal{F}_n(\theta) = 2\sum_{m=0}^{\infty}\binom{(1/n)-1}{2m}\binom{1/2}{m+1}[\tan(2\theta)]^{2m}. \tag{3.10}$$

This series converges only for $\theta < \pi/8$ and it is therefore not suitable for numerical evaluation in the case of maximal or nearly maximal mixing. It can be presented as a hypergeometric function

$$\mathcal{F}_n(\theta) = {}_2F_1\left(\frac{n-1}{2n}, \frac{2n-1}{2n}; 2; -\tan^2(2\theta)\right). \tag{3.11}$$

One can further use the Euler's formula to transform the function ${}_2F_1$ to an integral form [91],

$${}_2F_1(a,b;c;z) = \frac{\Gamma(c)}{\Gamma(b)\Gamma(c-b)}\int_0^1 dt\, t^{b-1}(1-t)^{c-b-1}(1-tz)^a, \tag{3.12}$$

suitable for numerical evaluation. By this analytical continuation the applicability of the results is extended to the range $0 \leq \theta \leq \pi/4$ [77].

In the extreme nonadiabatic limit, where $\gamma \ll 1$, the approximation made in deriving the formula (3.5) fails. The Landau-Zener method picks up only the leading term of the exponential, which is the dominant part for large γ. For a small γ there may be other contributions to the probability [90]. When $\gamma \to 0$, the formula (3.5) always gives $P_{LZ} \to 1$. However, for a quickly varying density, the level crossing probability should go to $\cos^2\theta$ [88]. A generalization of the LZ-formula appropriate for quickly varying density distributions is given by an ansatz [88]

$$P = \frac{e^{-\frac{\pi}{2}\gamma\mathcal{F}} - e^{-\frac{\pi}{2}\gamma\frac{\mathcal{F}}{\sin^2\theta}}}{1 - e^{-\frac{\pi}{2}\gamma\frac{\mathcal{F}}{\sin^2\theta}}}. \tag{3.13}$$

For a linear potential and small mixing angles this formula reduces to Eq. (3.5).

In Paper III of this thesis the Landau-Zener probabilities were evaluated by computing numerically the integral (3.4) and taking the extreme nonadiabatic limit (3.13) into account.

3.3 Multistate linear system and ICA

As mentioned, the original Landau-Zener analysis of level crossing concerned two-level systems with linear time-dependence (potential). A simple generalization of this is a system with an arbitrary number of crossing energy levels with a linear time-dependence. For a n-state system one needs to solve a differential equation of order n with time-dependent coefficient. An analytic solution for such a system has been obtained only for some special situations [89]. These include the equal slope case, when all but one unperturbed energy level have equal slope, as well as so-called bow tie case, where all levels have different slopes but they cross at the same point.

Independent crossing approximation (ICA)

It is intuitively evident that the probability for transitions in a multilevel system is obtained as a product of the two-state Landau-Zener probabilities if the crossings can be considered to occur independently, that is, the corresponding crossing regions are wide apart. Surprisingly enough, it has been shown numerically that for matrix elements corresponding to transitions between the lowest and the highest unperturbed energy state this method holds even if all crossing regions overlap. That is, the so-called independent crossing approximation (ICA) [89]

$$P_{kk} = \prod_{i=1}^{n} P_i^{LZ} \tag{3.14}$$

is valid for these transitions. In (3.14) n is the number of crossing points, P_i^{LZ} is the transition probability in the crossing point i handled as an independent two-level system. Here k denotes the unperturbed state with highest or lowest slope, and P_{kk} gives the probability for a system originally in one of these states to end up to the same state after all the crossing points are passed.

It is shown that the ICA holds for all exactly solvable cases with finite number of states [89]. It has been confirmed by many numerical checks. This has made some authors to believe, that a general multistate system can be solved in terms of two-state crossing probabilities of Landau and Zener [89, 92]. The validity of the ICA rule in the case of nonlinear

potential was tested in Paper III in the case of neutrinos and it was found to work really quite well.

Chapter 4

Effects of sterile neutrinos

As the solar neutrino puzzle has been beautifully solved and the atmospheric, reactor and beam neutrino experiments can be explained in terms of oscillations of the three active neutrinos, there is no compelling reason to introduce sterile neutrinos. However, sterile neutrinos may still exist. It is quite possible that the effects of sterile neutrinos, e.g. on the solar neutrino data, may have left hidden in the energy scale explored by SNO, which is sensitive only to the high energy tail of the solar neutrino spectrum. Sterile neutrinos might reveal themselves in the forthcoming sub-MeV experiments like CLEAN [56]. It is also possible that sterile neutrinos couple only to the state ν_3 which has practically no effect on the solar neutrino data.

In this Chapter a model with one or more sterile neutrinos is investigated. It is assumed that sterile neutrinos are nearly degenerate in mass with the active ones, a scenario which is still allowed by the current experiments. Predictions are made on how this kind of sterile neutrinos would reveal themselves in future experiments measuring the supernova and UHECR neutrino flux. Exploring sterile neutrinos in supernovae leads one to study also a more general problem of multistate nonlinear systems and the applicability of the Landau-Zener theory discussed in the previous Chapter.

4.1 Model with nearly degenerate sterile neutrinos

We now assume that in addition to the three active neutrinos ν_e, ν_μ and ν_τ there exist three sterile neutrinos, ν_{s1}, ν_{s2} and ν_{s3}. Let us assume that the active neutrinos mix mutually to

form three states $\hat{\nu}_i$,

$$\hat{\nu}_i = \sum_{l=e,\mu,\tau} U_{il}\nu_l, \tag{4.1}$$

where U is the standard 3×3 mixing matrix given in Eq. (1.2). In the absence of the sterile neutrinos, or if the sterile neutrinos decouple from the active ones, the states $\hat{\nu}_i$ would coincide with the mass eigenstate neutrinos of the SM. Suppose, however, that the sterile neutrinos ν_{si}, $i = 1, 2, 3$, do not decouple but they mix with the active ones according to

$$\begin{aligned} \nu_i &= \cos\varphi_i\, \hat{\nu}_i - \sin\varphi_i\, \nu_{si}, \\ \nu_i' &= \sin\varphi_i\, \hat{\nu}_i + \cos\varphi_i\, \nu_{si}. \end{aligned} \tag{4.2}$$

Then the neutrino mixing matrix (1.2) is extended to the form

$$U^{(6)} = \begin{pmatrix} \cos\varphi_1 U_{e1} & \cos\varphi_2 U_{e2} & \cos\varphi_3 U_{e3} & \sin\varphi_1 U_{e1} & \sin\varphi_2 U_{e2} & \sin\varphi_3 U_{e3} \\ \cos\varphi_1 U_{\mu 1} & \cos\varphi_2 U_{\mu 2} & \cos\varphi_3 U_{\mu 3} & \sin\varphi_1 U_{\mu 1} & \sin\varphi_2 U_{\mu 2} & \sin\varphi_3 U_{\mu 3} \\ \cos\varphi_1 U_{\tau 1} & \cos\varphi_2 U_{\tau 2} & \cos\varphi_3 U_{\tau 3} & \sin\varphi_1 U_{\tau 1} & \sin\varphi_2 U_{\tau 2} & \sin\varphi_3 U_{\tau 3} \\ -\sin\varphi_1 & 0 & 0 & \cos\varphi_1 & 0 & 0 \\ 0 & -\sin\varphi_2 & 0 & 0 & \cos\varphi_2 & 0 \\ 0 & 0 & -\sin\varphi_3 & 0 & 0 & \cos\varphi_3 \end{pmatrix}, \tag{4.3}$$

where U_{li}'s are the elements of the three neutrino mixing matrix of Eq. (1.2). The antineutrino states are assumed to mix similarly.

Obviously, this is not the most general way to mix the three sterile neutrinos with the three active ones. Firstly, in this scheme we have just three new mixing angles (φ_1, φ_2, φ_3) while in the most general case the number of additional angles would be 15. Secondly, we have not included any new CP-violation parameters, while in the general case 10 additional CP-phases would appear when one goes from the standard U to a 6×6 mixing matrix [4].

The neutrino states ν_i and ν_i' and the corresponding antineutrino states $\bar{\nu}_i$ and $\bar{\nu}_i'$ are the mass eigenstates with masses m_i and m_i', respectively. The mass spectrum of this system is illustrated in Fig. 4.1, where we have assumed the normal mass hierarchy. We have also indicated in the figure the effect of the active-sterile mixing (4.2) on the composition of the mass eigenstates with some arbitrarily chosen values for the mixing angles φ_i. The original research papers Paper I, Paper II and Paper IV of this thesis concern with this kind of mixing scheme and study its phenomenology in astrophysics.

We assume the mass difference of the states ν_i and ν_i' to be so small that in the processes studied in laboratory experiments, like particle decays $\mu \to e + \nu_e + \nu_\mu$ and $\pi, K \to l + \nu_l$,

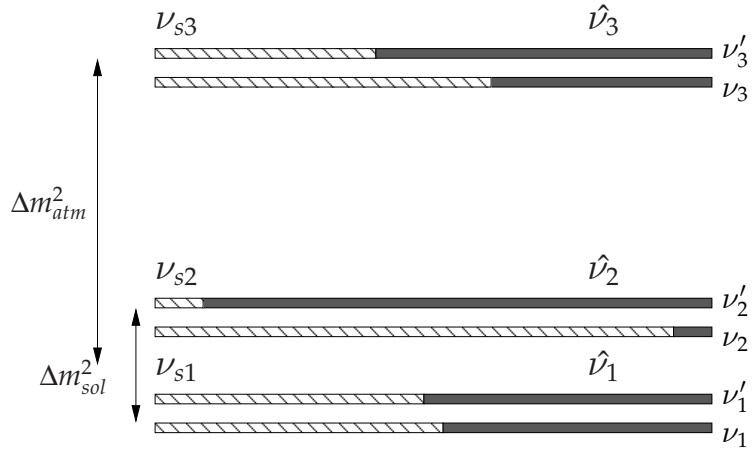

Figure 4.1: Mass states in a model with three sterile neutrinos, which are nearly degenerate with the active ones.

these two states are not distinguished but appear as a single state with couplings equal to those of the active state $\hat{\nu}_i$. There are models where degenerate neutrino pairs may naturally appear (see a discussion in section 1.3). To such models belongs the pseudo-Dirac model, where the mixing angles φ_i are close to the maximal value $\pi/4$.

This kind of active-sterile mixing would have remained unnoticed in the existing experiments, if the coupled mass states are nearly degenerate. The upper limits for the mass-squared differences $\Delta m^2_{ii'}$ ($i = 1, 2, 3$) between the eigenstates ν'_i and ν_i for this to happen are $\Delta m^2_{11'} < 10^{-12}$ eV^2, $\Delta m^2_{22'} < 10^{-11}$ eV^2 and $\Delta m^2_{33'} < 10^{-4}$ eV^2 [42]. The first two limits come from solar neutrino experiments, the third one from cosmology. If the values of the mixing angles φ_i are smaller than $\pi/4$, larger mass-squared differences would be allowed.

4.2 Effect on UHECR neutrino fluxes

Ultrahigh-energy cosmic ray (UHECR) neutrinos described in section 2.2 provide an excellent tool for exploring nearly degenerate sterile neutrinos, as is shown in Paper I. The huge distances to UHECR sources offer baselines, which can not be achieved in terrestrial experiments. They make it possible to test oscillations with Δm^2 down to 10^{-18} eV^2 [93]. In practice neutrinos travel in vacuum during their flight, leaving the leading role in their evolution to vacuum oscillations.

Sterile neutrinos can not be detected, but one can get information of their presence by

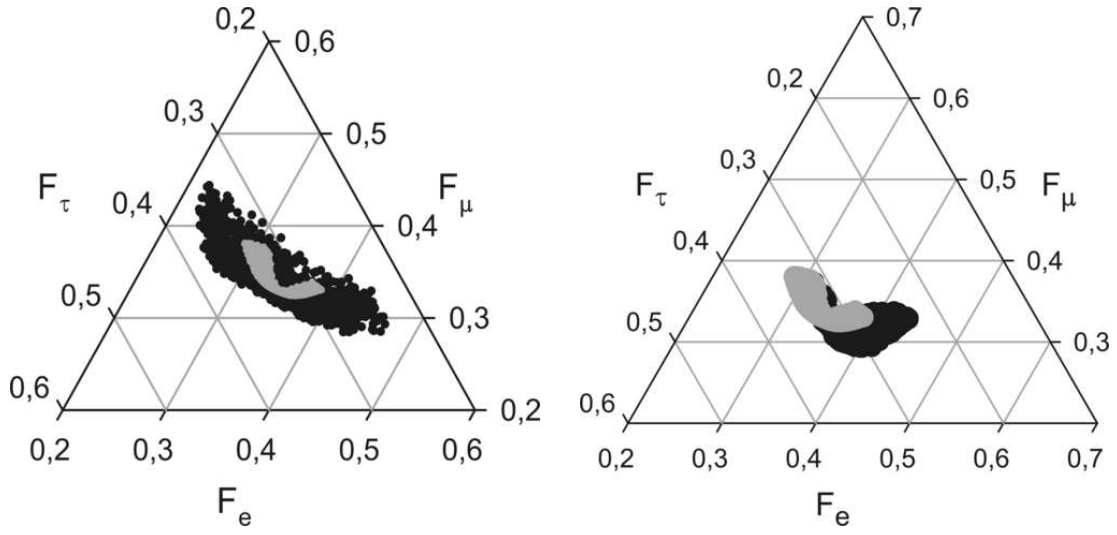

(a) 3 steriles (b) 1 sterile

Figure 4.2: Relative fluxes of the UHECR neutrinos at earth. The gray area corresponds to the situation with only active neutrinos present, corresponding mixing angles θ_{12}, θ_{23} and θ_{13} varying within their experimentally allowed ranges. The black area, in part behind the gray area, corresponds to the situation with (a) three sterile neutrinos with arbitrary mixing angles φ_i (b) one sterile neutrino mixed with the heaviest state with arbitrary mixing angle φ_3.

examining their effects on the relative fluxes F_l ,

$$F_l = \frac{\Phi_l}{\Phi_e + \Phi_\mu + \Phi_\tau}, \tag{4.4}$$

of the active neutrinos at the Earth. Here Φ_l denotes the measured flux of the neutrino flavor ν_l. In Paper I the values of the mixing angles θ_{ij} were allowed to vary within their experimentally allowed ranges. Bounds $0.49 < \theta_{12} < 0.67$, $0.63 < \theta_{23} < 0.94$ and $0 \leq \theta_{13} \leq 0.1$, each obtained from two-neutrino analysis, were used [69]. The first limit comes from combined solar and KamLAND reactor data [94], the second from atmospheric neutrino data [95] and the third from nonobservation of oscillations in CHOOZ [96] and Palo Verde [97] experiments. The allowed relative flux values given by these ranges of the mixing angles θ_{12}, θ_{23} and θ_{13} form the gray boomerang shaped area of Fig. 4.2(a).

If the mass-squared difference between the states in Eq. (4.2) is below 10^{-12} eV^2 the existence of the sterile flavor would have escaped detection in the oscillation experiments performed so far, but they could have measurable effects on the fluxes of the UHECR neutrinos

making the flux ratios to differ from those possible in the standard three active neutrino case. Allowing the active-sterile mixing angles φ_i vary freely within the range $0 \leq \varphi_i \leq \pi/4$ the black area of Fig. 4.2(a) is obtained, which shows that substantial deviations from the SM result (the gray area) are indeed possible.

The phenomenologically most interesting is the flux ratio of the electron and muon neutrinos,

$$R_{e\mu} \equiv \frac{F_\mathrm{e}}{F_\mu}\,. \tag{4.5}$$

In the case of three active neutrinos this ratio varies in the range

$$0.75 \lesssim (R_{e\mu})_\mathrm{SM} \lesssim 1.17\,, \tag{4.6}$$

when the mixing angles θ_{ij} vary in their experimentally allowed ranges, $0.49 < \theta_{12} < 0.67$, $0.63 < \theta_{23} < 0.94$ and $0 \leq \theta_{13} \leq 0.1$. In the presence of active-sterile mixing one has

$$0.47 \lesssim (R_{e\mu})_\mathrm{sterile} \lesssim 1.62\,. \tag{4.7}$$

The relative deviation of the ratio $R_{e\mu}$ from its SM value, caused by the active-sterile mixing, can have its value in the range

$$-40\% \lesssim \frac{(R_{e\mu})_\mathrm{sterile} - (R_{e\mu})_\mathrm{SM}}{(R_{e\mu})_\mathrm{SM}} \lesssim 70\%\,. \tag{4.8}$$

The largest positive deviation is achieved when the sterile mixing angle φ_1 is very small and the other two φ_2 an φ_3 are nearly maximal, while the largest negative deviation is obtained when φ_1 and φ_2 are nearly maximal and φ_3 is very small. In the former situation the flux ratios are approximatively $F_\mathrm{e} : F_\mu : F_\tau = 0.4 : 0.3 : 0.3$, in the latter situation $F_\mathrm{e} : F_\mu : F_\tau = 0.2 : 0.5 : 0.3$. The effect of the active-sterile mixing to the relative fluxes can thus be quite large and detectable in the future neutrino telescope experiments.

Let us consider the situation where there is only one sterile neutrino present. More specifically, let it be the state ν'_3, which has the loosest bounds from the solar neutrino data and might therefore have the largest effects on the flux ratio. In Fig. 4.2(b) a ternary plot corresponding to this situation is presented. As it is seen from the plot, even in this case of one sterile neutrino substantial deviations from the SM prediction are possible towards the direction of larger F_e and F_τ and smaller F_μ. In Fig. 4.3 the ratio $F_e/F_\mu = R_{e\mu}$ is plotted as a function of the active-sterile mixing angle φ_3, letting the ordinary mixing angles θ_{12}, θ_{23} and θ_{13} to vary within their experimental limits. As one can see, the allowed ranges of the sterile and non-sterile cases do not overlap when the active-sterile mixing angle is close to its maximal value.

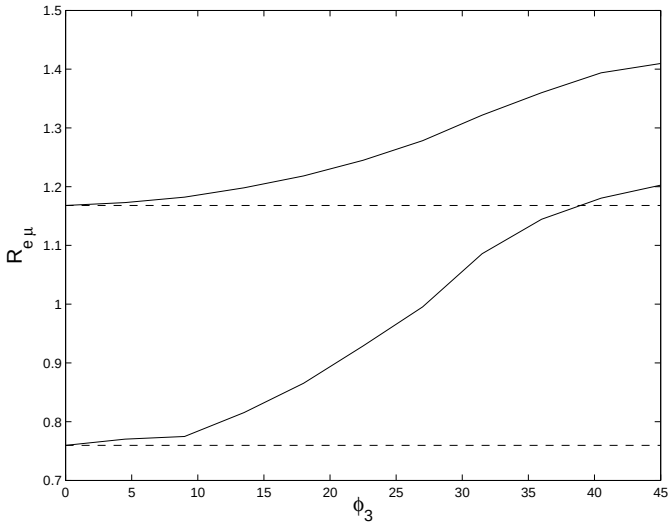

Figure 4.3: The ratio of electron and muon neutrino fluxes as a function of the active-sterile mixing angle φ_3. Only one sterile state ν_3' is present. The region between solid lines is the allowed range in the presence of ν_3' when the mixing angles θ_{12}, θ_{23} and θ_{13} are varied within their experimentally allowed values. The dashed lines correspond the situation in the SM case with no sterile neutrinos.

4.3 Effect on supernova neutrino fluxes

For supernova neutrinos, in contrast to the UHECR neutrinos, matter effects play the main role. This is because neutrinos are produced at high densities in the supernova core from where they travel through a medium with decreasing density to the surface of the star. In section 2.3 we discussed the matter effects in supernovae in the presence of three active neutrinos. In Fig. 4.4 energy levels of the system of three active (solid lines) and three sterile neutrinos (dashed lines) are presented. Note that we have used there the standard "normalization" of the matter effect where the effects caused by neutral current interactions are taken out of the Hamiltonian as a common factor. That is why the energy levels associated with the sterile neutrinos have an apparent dependence on the matter density in this plot.

As is seen from the Fig. 4.4, many additional crossings of energy levels appear when sterile neutrinos are present. Nevertheless, in the mixing scheme we are studying, presented in Eq. (4.2), only three of these crossings can lead to enhanced transitions between neutrino flavors (they are indicated by rings in Fig. 4.4). One of them (ν_1, ν_1') lies on the neutrino side

($N_e > 0$), while the other two (ν_2, ν_2' and ν_3, ν_3') lie in the antineutrino side ($N_e < 0$). Due to the small mass differences assumed between the states ν_i and ν_i', the new resonances occur at low densities, $\rho_R < 10^{-5}$ g $\cdot$ cm^{-3}, the exact value depending on the parameters $\Delta m^2_{ii'}$ and φ_i.

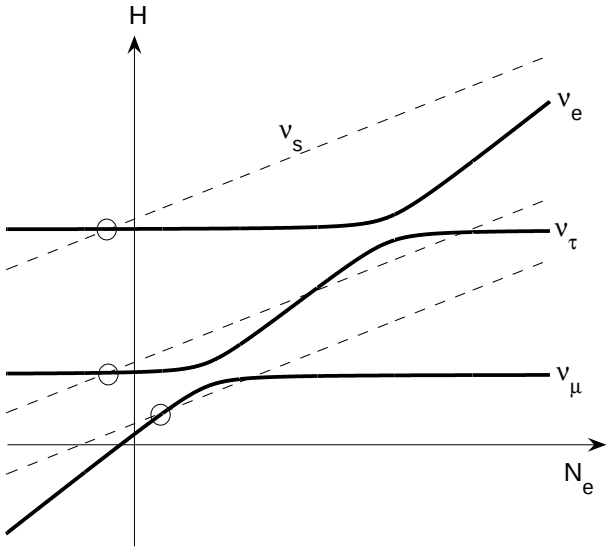

Figure 4.4: Neutrino eigenstates as a function of electron density, in the presence of three active neutrinos (solid line) and three sterile neutrinos (dashed line). For clarity the states are drawn as there were no active-sterile mixing. The crossings of states giving rise to enhanced transition in the case of the active-sterile mixing (4.2) are marked by circles.

A simplified LZ study

To find out the behavior of the energy states in the new resonances originating from the active-sterile mixing is a non-trivial task. One reason for this is that the matter potential has a power-law form instead of a linear behavior. In addition, the resonances overlap with each other in the low density region, where the L-resonance is still operative. Hence it is not a priori justified to use even the corrected LZ formula (3.8).

In Paper II, where this system was investigated, we first made a simplifying assumption that all the resonances between the active and sterile states are fully nonadiabatic. This is

rather conservative assumption, because in the nonadiabatic case the behavior of the states in an active-sterile resonance is like if there were no mixing at all. If the effects of the active-sterile mixing turned out to be measurable even in this conservative case, it would be promising to explore the system and the behavior in resonances in detail. In nonadiabatic case only the L- and H-resonances need to be considered, and they can be handled as separate two-state systems like in the case where only active neutrinos are present. When the active-sterile resonances are nonadiabatic, (anti)neutrinos always end up to the states ν_i at the surface of the supernova. These states contain a sterile component due to the active-sterile mixing.

The flavor composition of the neutrino flux on the surface of the star and at the Earth is given by

$$F_\alpha = \sum_{i=1}^{6} |U^{(6)}_{\alpha i}|^2 F_i, \tag{4.9}$$

where F_α is the relative flux of the flavor state ν_α ($\alpha = e, \mu, \tau, s1, s2, s3$) and F_i ($i = 1, 2, 3, 1', 2', 3'$) is the final occupation of the mass eigenstate ν_i. From Fig. 4.4 it can be deduced that $F_i = (F^0_x, F^0_e, F^0_x, 0, 0, 0)$ and $F_i = (F^0_x, F^0_x, F^0_e, 0, 0, 0)$ for a nonadiabatic and an adiabatic H-resonance, respectively. For antineutrinos an analogous formula is used with $\bar{F}_i = (F^0_{\bar{e}}, F^0_x, F^0_x, 0, 0, 0)$. In Paper II the analysis was done for two initial flux ratios, $F^0_e : F^0_{\bar{e}} : F^0_x = 4 : 3 : 2$ and $F^0_e : F^0_{\bar{e}} : F^0_x = 1 : 1 : 1$ (see discussion in section 2.3). The results are presented in Tables 4.1 and 4.2, where they are compared with the results of the three active neutrinos case.

In the study of Paper II the mixing angles θ_{12} and θ_{23} were fixed to the values $\theta_{12} = \pi/6$ and $\theta_{23} = \pi/4$. For the worse known θ_{13} two values were used, $\theta_{13} = 0$ and $\theta_{13} = \pi/32$, which both are within the allowed range ($\theta_{13} < 0.20$) obtained from the three-neutrino analysis of the present oscillation data. In respect to the transitions in the H-resonance, these two values of θ_{13} correspond to the two extreme cases of fully nonadiabatic ($P_H = 1$) and fully adiabatic ($P_H = 0$) transitions, respectively. The sterile mixing angles φ_i were allowed to vary freely. In the case of $F^0_e : F^0_{\bar{e}} : F^0_x = 1 : 1 : 1$ results are independent of the behavior of the states in the H-resonance. As sterile flavors can not be detected, the flux ratios of the active flavors are used as observables. We have chosen F_e/F_a, $F_{\bar{e}}/F_a$ and $F_e/F_{\bar{e}}$, where F_a is the sum of the fluxes of ν_μ, $\bar{\nu}_\mu$, ν_τ and $\bar{\nu}_\tau$.

From Tables 4.1 and 4.2 it is seen that the active-sterile mixing has measurable, albeit not outstanding, effects. In each case the flux ratios can either increase or decrease as compared with the SM prediction. A question arises, how the flux ratios would change if one or more of the active-sterile resonances turned out to be fully or partly adiabatic. This question was

	$P_H = 0$		$P_H = 1$	
	active	active + sterile	active	active + sterile
$\frac{F_e}{F_a}$	0.20	$0.13 - 0.30$	0.26	$0.19 - 0.35$
$\frac{F_{\bar{e}}}{F_a}$	0.27	$0.18 - 0.42$	0.28	$0.18 - 0.44$
$\frac{F_e}{F_{\bar{e}}}$	0.74	$0.71 - 0.78$	0.91	$0.81 - 1.07$

Table 4.1: Flux ratios F_e/F_a, $F_{\bar{e}}/F_a$ and $F_e/F_{\bar{e}}$ at the Earth in the case of an adiabatic ($P_H = 0$) and a nonadiabatic ($P_H = 1$) H-resonance. The active-sterile transitions are assumed to be nonadiabatic. The cases of active only and active + sterile are considered. The initial neutrino fluxes were assumed to have $F_e^0 : F_{\bar{e}}^0 : F_x^0 = 4 : 3 : 2$.

	active	active + sterile
$\frac{F_e}{F_a}$	0.25	$0.17 - 0.38$
$\frac{F_{\bar{e}}}{F_a}$	0.25	$0.17 - 0.38$
$\frac{F_e}{F_{\bar{e}}}$	1.00	1.00

Table 4.2: The same as in Table 4.1 but with the initial flux ratios $F_e^0 : F_{\bar{e}}^0 : F_x^0 = 1 : 1 : 1$. Now the ratios are independent of whether the H-resonance is adiabatic or nonadiabatic. The active-sterile transitions are assumed to be nonadiabatic. The cases of active only and active + sterile are considered.

addressed in Paper IV, where the evolution of neutrino states in supernova envelope was studied numerically in the presence of nearly degenerate sterile neutrinos.

Density matrix formalism

The evolution of a quantum system can be solved, at least in principle, as accurately as one wants by solving numerically the Schrödinger equation (3.1). If the system is in a mixed state, as is the case for supernova neutrinos, the density matrix formalism is a proper way to do that. The density matrix ρ is a kind of generalization for the state vector, and it allows to treat both pure and mixed systems on the same footing. The Schrödinger equation (3.1) is replaced by the equation

$$\dot{\rho} = i[\rho, H], \tag{4.10}$$

where the dot stands for time derivative. The density matrix is Hermitian and have positive eigenvalues, and it has $\mathrm{Tr}(\rho) = 1$. The diagonal elements of ρ give the occupation of different

states. Choosing the interaction states as basis states diagonal elements $\rho_{ll}(t)$ are just the normalized fluxes of different flavors at a given moment of time. The input needed are the initial fluxes and the Hamiltonian. In the case when only the three active neutrinos exist, $\rho(t)$ is a 3×3 matrix, and the initial fluxes are given as $\rho_{ll}(0) = F_l^0$, $l = e, \mu, \tau$. The Hamiltonian is of the form $H_m = H_0 + V$, where the effective potential takes into account the effects of matter and is given by Eq. (2.5). For the sterile neutrinos the effective potential is half of that given by Eq. (2.5). Antineutrinos are treated similarly, except that for them V has an opposite sign.

Solving (4.10) is in principle a straightforward numerical problem and it can be done by utilizing brute force. How demanding the solving actually is depends on the initial parameters and the degrees of freedom of the system. In the worst case the computation is time-consuming and also inaccurate because of round-off errors and instability.

Exact solution for supernova neutrinos

As discussed in section 4.1, the ν_3/ν_3' -mixing is practically not restricted by the solar neutrino data. Therefore it is reasonable to reduce the number of sterile states to one and consider only the ν_3/ν_3' -mixing. This choice also makes the computation more stable and less time consuming.

With our choice of mass hierarchy $m_{\nu_3'} > m_{\nu_3}$, the 33′-resonance lies in the antineutrino sector (see Fig. 4.4). Its effect is that the relative fraction of electronic flavors in comparison with the nonelectronic ones increases. Let us consider first the case of maximal mixing $\varphi = \pi/4$. In that case the ν_s/ν_3-resonance is totally adiabatic, and a neutrino born in the core as $\bar{\nu}_\tau$ leaves the star as ν_3'. This state is half active, half sterile, and the active part consists almost solely of the nonelectronic flavors ν_μ and ν_τ. Compared with the state $\hat{\nu}_3$, which is the final state in the SM case, the amount of the nonelectronic flavors is reduced, as a half of the state is now sterile. For an adiabatic H-resonance one has $F_e/F_a = 0.24$ and $F_{\bar{e}}/F_a = 0.35$, to be compared with the Standard Model values 0.17 and 0.24, respectively. For an nonadiabatic H-resonance one has $F_e/F_a = 0.35$ and $F_{\bar{e}}/F_a = 0.32$, to be compared with the Standard Model values 0.29 and 0.26, respectively.

In Paper IV the flux ratios were studied as a function of the active-sterile mixing angle φ. There the neutrino energy was fixed to $E = 10$ MeV, which corresponds to the maximal intensity of the neutrino flux. The initial fluxes were taken as $F_e^0 : F_{\bar{e}}^0 : F_x^0 = 4 : 2.3 : 1.2$, as given by the model of [75]. For neutrino parameters the global 3ν best-fit values $\Delta m_{12}^2 = 7.9 \cdot 10^{-5}\,\mathrm{eV}^2$, $\theta_{12} = 33.7^\circ$, $\Delta m_{23}^2 = 2.6 \cdot 10^{-3}\,\mathrm{eV}^2$, $\theta_{23} = 43.3^\circ$ and $\theta_{13} < 5.2^\circ$ [8] were used. The

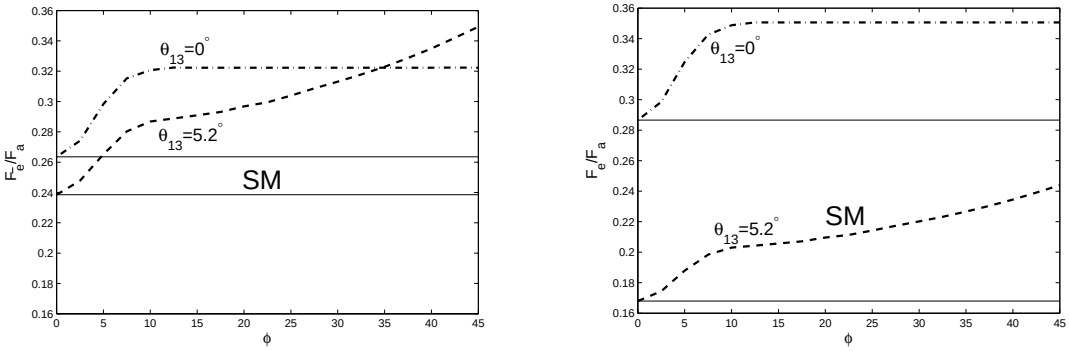

(a) $F_{\bar{e}}/F_a$ (b) F_e/F_a

Figure 4.5: Ratio of (a) $\bar{\nu}_e$ (b) ν_e and nonelectronic active fluxes as a function of sterile mixing angle φ_3. Results corresponding to minimum and maximum values of θ_{13} are presented. The horizontal lines indicate the limits of the active only (SM) case. Here $E = 10$ MeV.

active-sterile mass-squared difference was taken as $\Delta m^2_{33'} = 10^{-6}$ eV^2. Increasing of $\Delta m^2_{33'}$ from this value would not change the values of the final flux ratios, since the values saturate in this limit. As $\Delta m^2_{33'}$ decreases from this value the ratios F_e/F_a and $F_{\bar{e}}/F_a$ obtain smaller values at $\varphi = \pi/4$ than in the case of $\Delta m^2_{33'} = 10^{-6}$ eV^2. The sensitivity for φ disappears totally when $\Delta m^2_{33'} \leq 10^{-11}$ eV^2 and the same values for flux ratios are obtained as in the case of no active-sterile mixing.

To solve the density matrix equation (4.10) a variety of `MATLAB` solvers for ordinary differential equation were tested. An important feature of a suitable solver is that it should keep the trace of the density matrix as constant. Such a solver (`ode23s`), based on a modified Rosenbrock formula, was selected [98]. The density matrix equation (4.10) was solved for φ values from zero to its maximal value of $\pi/4$ at intervals of 2.5°. Because the adiabaticity of H-resonance has a notable impact on the final fluxes, we checked both adiabatic and nonadiabatic cases, using upper and lower limits of the mixing angle θ_{13}. Because the fraction of the ν_e and $\bar{\nu}_e$ on states ν_3 and ν'_3 is negligible, the ratio $F_e/F_{\bar{e}}$ is insensitive to the ν_3/ν'_3 -mixing. Hence the evolution of the flux ratios $F_{\bar{e}}/F_a$ and F_e/F_a was followed, as shown in Fig. 4.3.

Using a two-state approximation, i.e. calculating the transition probability from (3.8) with (3.7), the 33′-resonance is nonadiabatic when $\varphi \lesssim 12°$. Then $\bar{\nu}_\tau$ ends up to state ν_3, which has a sterile fraction proportional to $\sin^2\varphi$. As φ increases from zero to 12° the sterile fraction increases, decreasing the weight of nonelectronic flavors ν_μ and ν_τ in that state. As a consequence the ratios $F_{\bar{e}}/F_a$ and F_e/F_a increase.

Let us now consider the parameter region $\varphi \gtrsim 12^\circ$ where the $33'$-resonance is fully adiabatic. Then a neutrino born as $\bar{\nu}_\tau$ ends up to the state ν_3' with sterile fraction proportional to $\cos^2\varphi$, decreasing with increasing φ. The ratios $F_{\bar{e}}/F_a$ and F_e/F_a seem to either saturate or increase when φ increases. This behavior can be understood as follows.

In the case of $\theta_{13} = 0$, the H-resonance is nonadiabatic. The flux originating at the state ν_τ ends up to the state ν_3 whereas the flux originating as $\bar{\nu}_\tau$ goes to the state ν_3'. These fluxes have an equal original weight, $F_x^0 = 1.2$. As φ increases, the sterile component of the state ν_3 increases but at the same time the sterile component of the state ν_3' decreases by same amount. So there is no net effect and the flux ratios $F_{\bar{e}}/F_a$ and F_e/F_a saturate to constant values.

When $\theta_{13} = 5.2^\circ$ the H-resonance is fully adiabatic. Considering the pair ν_3, ν_3' there is in this case more flow to the state ν_3 because it is occupied by neutrinos born as ν_e which have a large relative initial weight, $F_e^0 = 4$. Now the increase of the sterile component in state ν_3 overrides its reduction in state ν_3' and the net effect is that the ratios $F_{\bar{e}}/F_a$ and F_e/F_a keep increasing as the angle φ increases.

The bands due to uncertainty of the value of the mixing angle θ_{13} in Fig. 4.5 are wider for the flux ratio F_e/F_a than for $F_{\bar{e}}/F_a$. This is because the mixing angle θ_{13} has more effect on the flux of ν_e than on that of $\nu_{\bar{e}}$, because the H-resonance lies in the neutrino sector in the normal hierarchy case we are considering. The ratio $F_{\bar{e}}/F_a$ seems to offer a quite promising test for the active-sterile mixing. Even for relatively small mixing the ratio might deviate substantially from its value in the case of three active neutrinos. For $\varphi > 5^\circ$ this effect could be seen independently of the unknown mixing angle θ_{13}.

4.4 Validity of ICA for three states in nonlinear potential

The level crossing in multilevel system is a problem one encounters in many branches of physics. This problem, also known as multilevel Landau-Zener problem, in particular in quantum optics and atomic physics. As discussed in Chapter 3, the basic question is whether the Landau-Zener theory of two-level systems is applicable in the systems where there are overlapping resonances. It has been shown analytically and by numerical studies that for linearly varying energy levels one can successfully present level crossing probabilities as products of the appropriate two-level LZ probabilities even if the two-level crossing regions overlap. This question is addressed in Paper III where three-level system with a nonlinear time dependence is studied.

A shortcoming of the numerical approach made in section 4.3 is that one does not achieve a detailed information of the behavior of the system. Instead the system is dealt as a black box, where a certain input leads a certain output. A detailed information of the system, i.e. understanding what is going on in a particular resonance, would also help one to analyze the experimental data. Therefore it would be useful to search for a physically more revealing and computationally less heavy way to study the system. This is what is done in Paper III.

In Paper III the effects of overlapping resonances were studied in a neutrino system by considering a toy model with three states with different interactions in a nonlinear potential. The aim was to investigate whether the independent crossing approximation rule discussed in section 3.3 is applicable also in this nonlinear case. This question has not been previously studied but all the earlier studies has concerned with linear cases. To test the validity of ICA the results obtained numerically by the density matrix formalism were used as reference values.

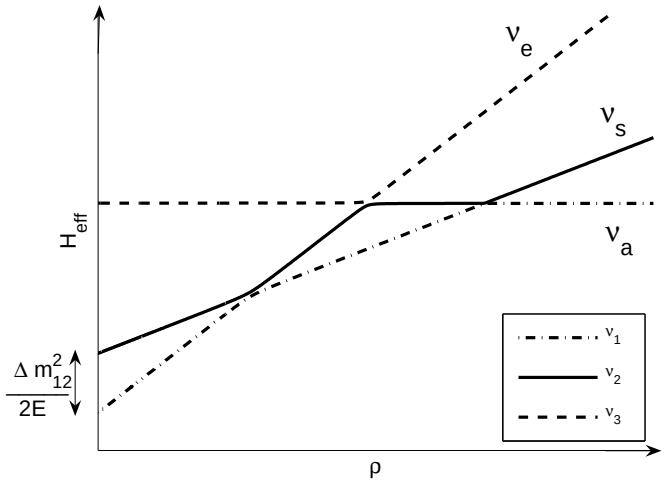

Figure 4.6: Energy levels of system consisting of ν_e (the steepest straight line), ν_s (the next steepest line) and ν_a (the horizontal line).

The toy model includes the electron neutrino ν_e, a sterile neutrino ν_s, and a nonelectronic active neutrino ν_a which all behave differently in matter. The energy levels of the system are shown in Fig. 4.6. According to (1.13) the effective potentials of ν_e, ν_s and ν_a in matter are $V_e = \sqrt{2}G_F N_e$, $V_a = 0$ and $V_s = \frac{1}{\sqrt{2}}G_F N_e$, where the neutral current contributions are subtracted and $N_n = N_e$ is assumed. Neutrino mixing parameters were deliberately chosen

so that the resonances 32 and 21 are semiadiabatic. For small values of Δm^2_{12} the resonances are separated but as the value of Δm^2_{12} increases the resonances start to overlap. The transition probabilities of the resonances were calculated by using (3.4). The total probability P^{LZ}_{31} for transition from the highest energy state ν_3 to the lowest one ν_1 was obtained by multiplying these two probabilities $P^{LZ}_{31} = P^{LZ}_{32} P^{LZ}_{21}$. This ICA result was then compared with the numerical result P^{ρ}_{31} obtained by using the density matrix approach. In Fig. 4.7 the both probabilities are presented as a function of the squared mass difference Δm^2_{12} of the states ν_1 and ν_2 in vacuum.

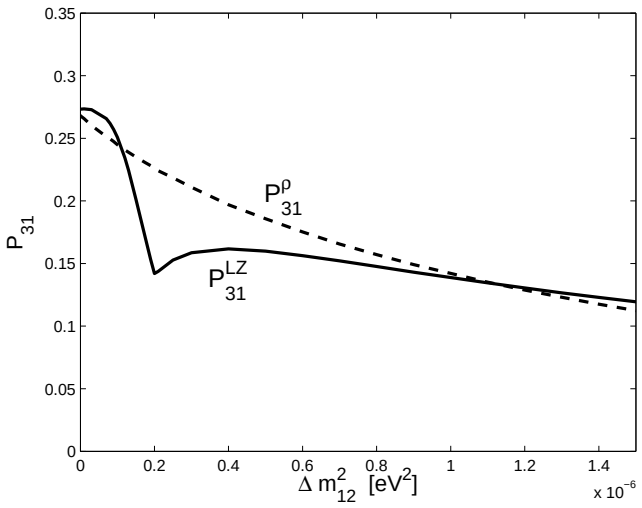

Figure 4.7: The probability for transition $3 \to 1$ as a function of Δm^2_{12} calculated by using the LZ-theory (solid line) and density matrix formalism (dashed line).

The transition regions (1.17) of the 32 and 21 crossings start to overlap at $\Delta m^2_{12} = 0.2 \cdot 10^{-6}\,\mathrm{eV}^2$ and the overlap is maximal at $\Delta m^2_{12} = 0.5 \cdot 10^{-6}\,\mathrm{eV}^2$, where the transition points coincide. At $\Delta m^2_{12} = 1 \cdot 10^{-6}\,\mathrm{eV}^2$ transition regions have passed each other and are separated again. The Landau-Zener model seems to work rather well in the $V \sim t^{-3}$ case, except in a region around a curious dip at $\Delta m^2_{12} = 0.2 \cdot 10^{-6}\,\mathrm{eV}^2$. The dip is actually an artifact caused by simplistic use of LZ-theory, as will be explained in the following.

In Eq. (3.4) the upper limit of the integral corresponds to the zero of the integrand. It is chosen to be the branch point in the upper half-plane of the complex time that is closest to the real axis as was explained earlier.

What happens in the case studied in Paper III is that at $\Delta m^2_{12} = 0.2 \cdot 10^{-6}\,\mathrm{eV}^2$ there are

two branch points with equal imaginary parts, and a role of the closest branch point moves from one branch point to the other at this value of Δm^2_{12}. That is, a different branch point gives the dominant contribution to P_{31} for large values than for small values of Δm^2_{12}. This is shown in Fig. 4.8, where P_{31} is plotted for both of these values. Obviously, the contribution of both zeros should be taken into account when evaluating P_{31}. For a two-level case the both zeros might be taken into account coherently, as was discussed in [99] in a totally different physical situation of quantum optics. The incoherent sum obviously gives a too large result as it neglects interference effects. It is a subject of a further study to find out how the coherent summation should be done in a three-level case, where the result of [99] is not applicable.

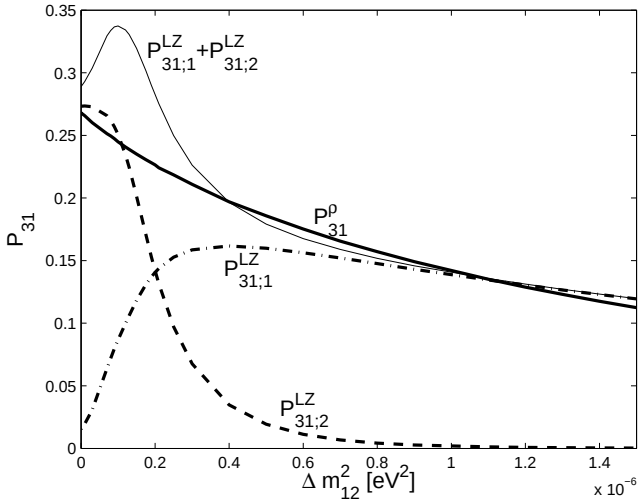

Figure 4.8: The contributions corresponding to the two dominating branch points $(t_0)_1$ and $(t_0)_2$ to the transition probability P_{31} (dash-dotted and dashed lines, respectively). Also shown are the numerical result obtained numerically by density matrix approach (thick solid line) and the incoherent sum of the contributions from the two branch points (thin solid line).

Summary

The aim of this study was to explore signals of sterile neutrinos from astrophysical sources. The physics of ultrahigh-energy neutrinos born in active galactic nuclei (AGN) and gamma ray bursts (GRBs) and supernova neutrinos were studied as a possible environment to test the hypothesis that there exists in Nature three sterile neutrinos nearly degenerate with the known active neutrinos. The sterile neutrinos were assumed to mix pairwise with the active neutrino mass eigenstates. The current values for the ordinary neutrino mixing parameters from neutrino oscillation experiments were used, while the values of the active-sterile mixing angles were allowed to vary with no restrictions. Astrophysical neutrinos were found to offer a suitable probe for studying the existence of such sterile neutrinos.

In the case of ultrahigh-energy neutrinos the oscillations will average out. It turned out that the active-sterile neutrino mixing would change the active neutrino flux ratios detected at the Earth.

In supernovae matter effects on the evolution of neutrino states play an important role. Neutrino mixing angles and eigenstates are functions of density of the background matter. In medium with varying density the Mikheyev-Smirnov-Wolfenstein effect takes place and an enhanced flavor conversion happens in resonance regions. The possible active-sterile mixing increases the number of resonances as compared with the standard three neutrino case. In this thesis the Landau-Zener approximation for level crossing probabilities as well as the density matrix formalism were used to find out the active neutrino flux ratios at the Earth. To improve the precision of supernova neutrino signals a more detailed information about the initial neutrino fluxes is needed.

When considering supernova neutrinos, a Landau-Zener problem of three states in non-linear potential was met. A general analytic solution for such a problem does not exist. The validity of independent crossing approximation (ICA) suitable in the case of linear potential was tested in this nonlinear case and it was found that the ICA works well.

Detecting UHECR neutrinos is still a challenge for experimentalists. The fluxes are low and atmospheric neutrinos pose a substantial background. From Milky Way supernova the existing neutrino detectors, like the Super-Kamiokande, would detect thousands of events. However, the energy spectrum is currently detectable only for electron antineutrinos. In suggested forthcoming experiments like CLEAN the energy information also of the nonelectronic neutrino flavors would be available.

Bibliography

[1] S. M. Bilenky and B. Pontecorvo, Phys. Rept. **41**, 225 (1978).

[2] ALEPH, S. Schael *et al.*, Phys. Rept. **427**, 257 (2006), hep-ex/0509008.

[3] Z. Maki, M. Nakagawa, and S. Sakata, Prog. Theor. Phys. **28**, 870 (1962).

[4] C. W. Kim and A. Pevsner, *Neutrinos in Physics and Astrophysics* (Harwood Academic Publishers, 1993).

[5] J. Bonn *et al.*, Nucl. Phys. Proc. Suppl. **91**, 273 (2001).

[6] V. M. Lobashev *et al.*, Nucl. Phys. Proc. Suppl. **91**, 280 (2001).

[7] C. Kraus *et al.*, Eur. Phys. J. C **40**, 447 (2005), hep-ex/0412056.

[8] M. C. Gonzalez-Garcia and M. Maltoni, (2007), arXiv:0704.1800 [hep-ph].

[9] Super-Kamiokande, Y. Fukuda *et al.*, Phys. Rev. Lett. **81**, 1562 (1998), hep-ex/9807003.

[10] SNO, Q. R. Ahmad *et al.*, Phys. Rev. Lett. **89**, 011301 (2002), nucl-ex/0204008.

[11] KamLAND, K. Eguchi *et al.*, Phys. Rev. Lett. **90**, 021802 (2003), hep-ex/0212021.

[12] K2K, M. H. Ahn *et al.*, Phys. Rev. D **74**, 072003 (2006), hep-ex/0606032.

[13] MINOS, D. G. Michael *et al.*, Phys. Rev. Lett. **97**, 191801 (2006), hep-ex/0607088.

[14] L. Wolfenstein, Phys. Rev. D **17**, 2369 (1978).

[15] H. W. Zaglauer and K. H. Schwarzer, Z. Phys. C **40**, 273 (1988).

[16] A. Y. Smirnov, (2003), hep-ph/0305106.

[17] S. P. Mikheev and A. Y. Smirnov, Sov. J. Nucl. Phys. **42**, 913 (1985).

[18] L. Landau, Physik. Z. Sowjet. **2**, 46 (1932).

[19] C. Zener, Proc. Roy. Soc. Lond. **A137**, 696 (1932).

[20] R. R. Volkas, Prog. Part. Nucl. Phys. **48**, 161 (2002), hep-ph/0111326.

[21] G. Altarelli and F. Feruglio, (1999), hep-ph/9905536.

[22] P. Minkowski, Phys. Lett. B **67**, 421 (1977).

[23] M. Gell-Mann, P. Ramond, and R. Slansky, *Supergravity* (North Holland, Amsterdam, 1979).

[24] T. Yanagida, In Proceedings of the Workshop on the Baryon Number of the Universe and Unified Theories, Tsukuba, Japan, 13-14 Feb 1979.

[25] D. Chang and O. C. W. Kong, Phys. Lett. B **477**, 416 (2000), hep-ph/9912268.

[26] P. Q. Hung, Phys. Rev. D **67**, 095011 (2003), hep-ph/0210131.

[27] Z. G. Berezhiani and R. N. Mohapatra, Phys. Rev. D **52**, 6607 (1995), hep-ph/9505385.

[28] T. D. Lee and C.-N. Yang, Phys. Rev. **104**, 254 (1956).

[29] R. Foot, H. Lew, and R. R. Volkas, Phys. Lett. B **272**, 67 (1991).

[30] A. Salam, Nuovo Cim. **5**, 299 (1957).

[31] V. Berezinsky, M. Narayan, and F. Vissani, Nucl. Phys. B **658**, 254 (2003), hep-ph/0210204.

[32] D. N. Schramm and M. S. Turner, Rev. Mod. Phys. **70**, 303 (1998).

[33] R. Barbieri and A. Dolgov, Phys. Lett. B **237**, 440 (1990).

[34] R. Barbieri and A. Dolgov, Nucl. Phys. B **349**, 743 (1991).

[35] K. Kainulainen, Phys. Lett. B **244**, 191 (1990).

[36] K. Enqvist, K. Kainulainen, and J. Maalampi, Phys. Lett. B **249**, 531 (1990).

[37] K. Enqvist, K. Kainulainen, and M. J. Thomson, Nucl. Phys. B **373**, 498 (1992).

[38] X.-D. Shi and G. M. Fuller, Phys. Rev. Lett. **83**, 3120 (1999), astro-ph/9904041.

[39] LSND, A. Aguilar *et al.*, Phys. Rev. D **64**, 112007 (2001), hep-ex/0104049.

[40] A. Strumia, Phys. Lett. B **539**, 91 (2002), hep-ph/0201134.

[41] The MiniBooNE, A. A. Aguilar-Arevalo *et al.*, (2007), arXiv:0704.1500 [hep-ex].

[42] M. Cirelli, G. Marandella, A. Strumia, and F. Vissani, Nucl. Phys. B **708**, 215 (2005), hep-ph/0403158.

[43] J. N. Bahcall, A. M. Serenelli, and S. Basu, Astrophys. J. Suppl. **165**, 400 (2006), astro-ph/0511337.

[44] J. N. Bahcall and C. Pena-Garay, New J. Phys. **6**, 63 (2004), hep-ph/0404061.

[45] J. Davis, Raymond, D. S. Harmer, and K. C. Hoffman, Phys. Rev. Lett. **20**, 1205 (1968).

[46] SAGE, J. N. Abdurashitov *et al.*, Phys. Rev. C **60**, 055801 (1999), astro-ph/9907113.

[47] GALLEX, W. Hampel *et al.*, Phys. Lett. B **447**, 127 (1999).

[48] GNO, M. Altmann *et al.*, Phys. Lett. B **616**, 174 (2005), hep-ex/0504037.

[49] Kamiokande, Y. Fukuda *et al.*, Phys. Rev. Lett. **77**, 1683 (1996).

[50] Super-Kamiokande, S. Fukuda *et al.*, Phys. Rev. Lett. **86**, 5651 (2001), hep-ex/0103032.

[51] J. N. Bahcall, Phys. Scripta **T121**, 46 (2005), hep-ph/0412068.

[52] J. N. Bahcall, A. M. Serenelli, and S. Basu, Astrophys. J. **621**, L85 (2005), astro-ph/0412440.

[53] A. Bandyopadhyay, S. Choubey, S. Goswami, S. T. Petcov, and D. P. Roy, Phys. Lett. B **608**, 115 (2005), hep-ph/0406328.

[54] Borexino, C. Arpesella *et al.*, Phys. Lett. B **658**, 101 (2008), arXiv:0708.2251 [astro-ph].

[55] A. Strumia, Nucl. Phys. Proc. Suppl. **143**, 144 (2005), hep-ph/0407132.

[56] D. N. McKinsey and K. J. Coakley, Astropart. Phys. **22**, 355 (2005), astro-ph/0402007.

[57] E. Waxman and J. N. Bahcall, Phys. Rev. Lett. **78**, 2292 (1997), astro-ph/9701231.

[58] V. Berezinsky, Nucl. Phys. Proc. Suppl. **151**, 260 (2006), astro-ph/0505220.

[59] P. Bhattacharjee and G. Sigl, Phys. Rept. **327**, 109 (2000), astro-ph/9811011.

[60] S. Pakvasa, Venice 2003, Neutrino telescope, vol. 2 , 469 (2003), hep-ph/0305317.

[61] L. Bento, P. Keränen, and J. Maalampi, Phys. Lett. B **476**, 205 (2000), hep-ph/9912240.

[62] H. Athar, M. Jezabek, and O. Yasuda, Phys. Rev. D **62**, 103007 (2000), hep-ph/0005104.

[63] K. Giesel, J. H. Jureit, and E. Reya, Astropart. Phys. **20**, 335 (2003), astro-ph/0303252.

[64] The IceCube, J. Ahrens *et al.*, Nucl. Phys. Proc. Suppl. **118**, 388 (2003), astro-ph/0209556.

[65] ANTARES, E. Aslanides *et al.*, (1999), astro-ph/9907432.

[66] NESTOR, S. E. Tzamarias, Nucl. Instrum. Meth. **A502**, 150 (2003).

[67] J. F. Beacom, N. F. Bell, D. Hooper, S. Pakvasa, and T. J. Weiler, Phys. Rev. D **68**, 093005 (2003), hep-ph/0307025.

[68] J. F. Beacom, N. F. Bell, D. Hooper, S. Pakvasa, and T. J. Weiler, Phys. Rev. Lett. **90**, 181301 (2003), hep-ph/0211305.

[69] G. Barenboim and C. Quigg, Phys. Rev. D **67**, 073024 (2003), hep-ph/0301220.

[70] J. F. Beacom *et al.*, Phys. Rev. Lett. **92**, 011101 (2004), hep-ph/0307151.

[71] S. M. Bilenky, C. Giunti, J. A. Grifols, and E. Masso, Phys. Rept. **379**, 69 (2003), hep-ph/0211462.

[72] KAMIOKANDE-II, K. Hirata *et al.*, Phys. Rev. Lett. **58**, 1490 (1987).

[73] R. M. Bionta *et al.*, Phys. Rev. Lett. **58**, 1494 (1987).

[74] T. Totani, K. Sato, H. E. Dalhed, and J. R. Wilson, Astrophysical Journal **496**, 216 (1998).

[75] G. G. Raffelt, M. T. Keil, R. Buras, H.-T. Janka, and M. Rampp, Kanazawa 2003, Neutrino oscillations and their origin , 380 (2003), astro-ph/0303226.

[76] K. Nomoto and M. Hashimoto, Phys. Rep. **163**, 13 (1988).

[77] M. Kachelriess, A. Strumia, R. Tomas, and J. W. F. Valle, Phys. Rev. **D65**, 073016 (2002), hep-ph/0108100.

[78] G. L. Fogli, E. Lisi, D. Montanino, and A. Palazzo, Phys. Rev. D **65**, 073008 (2002), hep-ph/0111199.

[79] C. Lunardini, Contribution to the 11th Annual International Conference on Supersymmetry and the Unification of Fundamental Interaction (SUSY 2003) , Tucson, Arizona, hep-ph/0307257.

[80] K. Takahashi, K. Sato, H. E. Dalhed, and J. R. Wilson, Astropart. Phys. **20**, 189 (2003), astro-ph/0212195.

[81] C. Lunardini and A. Y. Smirnov, JCAP **0306**, 009 (2003), hep-ph/0302033.

[82] A. Burrows, J. Hayes, and B. A. Fryxell, Astrophys. J. **450**, 830 (1995), astro-ph/9506061.

[83] C. Lunardini and A. Y. Smirnov, Astropart. Phys. **21**, 703 (2004), hep-ph/0402128.

[84] A. S. Dighe, M. Kachelriess, G. G. Raffelt, and R. Tomas, JCAP **0401**, 004 (2004), hep-ph/0311172.

[85] H. Nakamura, *Nonadiabatic transitions. Concepts, Basic Theories and Applications* (World Scientific, 2002).

[86] C. E. Carroll and H. F. T., J. Phys. A: Math. Gen. **19**, 2061 (1986).

[87] S. J. Parke, Phys. Rev. Lett. **57**, 1275 (1986).

[88] T.-K. Kuo and J. T. Pantaleone, Phys. Rev. D **39**, 1930 (1989).

[89] S. Brundobler and V. Elser, J. Phys. A: Math. Gen. **26**, 1211 (1993).

[90] L. Landau and E. Lifshitz, *Quantum mechanics: Nonrelativistic theory* (Pergamon, 1977).

[91] S. Hassani, *Mathematical Physics* (Springer, 2002).

[92] A. V. Shytov, Phys. Rev. A **70**, 052708 (2004), cond-mat/0312011.

[93] S. Pakvasa, Nucl. Phys. Proc. Suppl. **137**, 295 (2004), hep-ph/0412371.

[94] P. C. de Holanda and A. Y. Smirnov, JCAP **0302**, 001 (2003), hep-ph/0212270.

[95] J. N. Bahcall, M. C. Gonzalez-Garcia, and C. Pena-Garay, JHEP **02**, 009 (2003), hep-ph/0212147.

[96] CHOOZ, M. Apollonio *et al.*, Phys. Lett. B **466**, 415 (1999), hep-ex/9907037.

[97] F. Boehm *et al.*, Phys. Rev. D **64**, 112001 (2001), hep-ex/0107009.

[98] L. F. Shampine and M. Reichelt, SIAM Journal on Scientific Computing **18**, 1 (1997).

[99] N. V. Vitanov and K. A. Suominen, Phys. Rev. A **59**, 4580 (1999).